CHALMERS
UNIVERSITY OF TECHNOLOGY

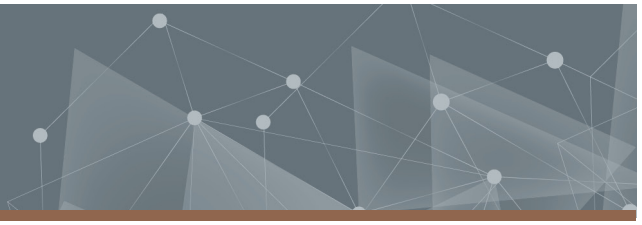

Richardson models for mesoscopic pairing interactions

Master's thesis in Master Programme Physics

FABIAN RESARE

DEPARTMENT OF PHYSICS

CHALMERS UNIVERSITY OF TECHNOLOGY
Gothenburg, Sweden 2022
www.chalmers.se

Master's thesis 2022

Richardson models for mesoscopic pairing interactions

FABIAN RESARE

CHALMERS
UNIVERSITY OF TECHNOLOGY

Department of Physics
Chalmers University of Technology
Gothenburg, Sweden 2022

Richardson models for mesoscopic pairing interactions
FABIAN RESARE

Supervisor: Johannes Hofmann, Department of Physics, Gothenburg University
Examiner: Ulf Gran, Department of Physics, Chalmers University of Technology

Master's Thesis 2022
Department of Physics
Chalmers University of Technology
SE-412 96 Gothenburg
Telephone +46 31 772 1000

Typeset in LaTeX
Printed by Chalmers Reproservice
Gothenburg, Sweden 2022

Richardson models for mesoscopic pairing interactions
FABIAN RESARE
Department of Physics
Chalmers University of Technology

Abstract

Pairing interactions in quantum mechanics have previously been used to model a wide variety of systems, including nuclear physics and superconductors. A main benefit of such models is that they, unlike many other popular interaction models, are integrable. This enables pairing problems to be solved exactly at a comparatively low computational cost. In this thesis, such models have been employed to study the mesoscopic physics of superconductors and harmonically trapped ultracold atoms. An numerical algorithm was developed to solve the pairing models, and obtain exact solutions for arbitrary excited states and single-particle spectra. This has enabled producing excitation spectra for significantly larger systems of trapped atoms than what was previously possible, and has led to a greater understanding of previous observed experimental data. A prediction for the functional dependence of the minimal first pair excitation energy has been obtained, which future experiments should be able to test.

Keywords: Richardson models, superconductivity, mesoscopic physics, ultracold quantum gases.

Acknowledgements

I would like to thank my supervisor Johannes for his help in introducing me to the field of mesoscopic quantum gases and for his input during the project. I would also like to thank my examiner Ulf for taking the time to review my work. Additionally I would also like to thank my fellow thesis workers for discussions and for making the project a lot more enjoyable.

Finally I would also like to acknowledge the contributors to the open source tools and libraries which this thesis has made use of, without which I would not have gotten a lot done.

Fabian Resare, Gothenburg, 2022

Contents

1
Introduction

1.1 Quantum mechanics and integrable models

Ever since its inception in the early 1900s, quantum mechanics has proved a successful description of microscopic physics. For the purposes of this thesis, quantum mechanics can be formulated in the Schrödinger picture by taking that the time evolution of states $|\psi(0)\rangle$ is governed by the Hamiltonian operator H. One has then that

$$|\psi(t)\rangle = e^{-iHt/\hbar} |\psi(0)\rangle \tag{1.1}$$

By deriving with respect to t, the Schrödinger equation

$$H |\psi(t)\rangle = -i\hbar \frac{d}{dt} |\psi(t)\rangle \tag{1.2}$$

is found. There are many systems for which the Hamiltonian is known, with for example the Hamiltonian of N free particles being

$$H = -\sum_{j=1}^{N} \frac{\hbar^2}{2m} \nabla_j^2. \tag{1.3}$$

Such a non-interacting Hamiltonian has well-known eigenstates, which can be labelled by the individual particle momenta $\mathbf{k}_1$ through $\mathbf{k}_N$, giving

$$H |\mathbf{k}_1, \mathbf{k}_2, ..., \mathbf{k}_N\rangle = \sum_{j=1}^{N} \frac{\hbar^2 |\mathbf{k_j}|^2}{2m} |\mathbf{k}_1, \mathbf{k}_2, ..., \mathbf{k}_N\rangle . \tag{1.4}$$

From equation (1.1), one notes that eigenstates of the Hamiltonian evolve only with a phase. This means that their eigenvalues are constants of motion. These constants of motion, E, are the possible obeservable energies of the system and the set of possible energies is called the spectrum of the theory. Measuring energy spectra experimentally is often the way to assess the validity of quantum mechanical models.

A hindrance in the understanding of quantum mechanics is that many models of interaction between particles are not analytically solvable. In order to obtain predicitons one must turn to numerical methods, often together with approximations, to be able to produce results. Such methods have been used with great success historically, but unfortunately a great deal of the known physically interesting models become computationally unfeasible to solve numerically for even moderately sized systems. It is thus of great interest to find physically descriptive models which can be analytically solved, so called integrable models.

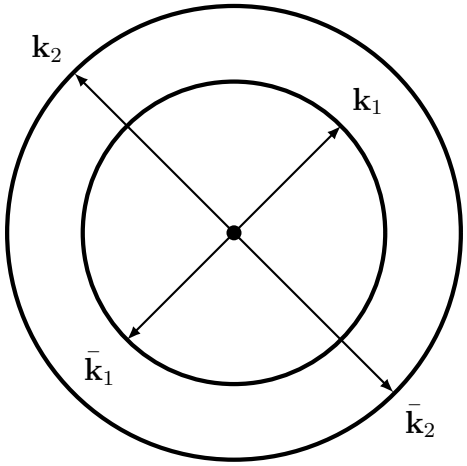

Figure 1.1: A sketch of the transition enabled by the pairing interaction between Cooper pairs of time-reversed particles at different momentum shells, the radius of the sketch denoting $|\mathbf{k}|$.

1.2 Pairing models and superconductivity

Pairing models were first introduced by Bardeen, Cooper and Schrieffer (BCS) [1] in their explanation of superconductivity and modifies the theory of free quantum gases to include a pairing interaction. Such an interaction assumes that the particles form Cooper pairs, consisting of particles with opposite momenta and spin. Such pairs will have net zero momentum and even if the individual particles are fermions, the Cooper pairs will have integer spin and appear as composite bosons. Cooper originally showed that such pairs will condense for an arbitrarily small pairing attraction [2], for electrons situated at the Fermi surface of opposite spin. Figure 1.1 shows a sketch of this transitions enabled by the interaction.

In section 2.1, it is shown that the pairing interaction in the second quantised formalism is equivalent to a contact interaction in position space. This provides a physical interpretation of the pairing interaction as a zero-range interaction between point particles, which in the case of electron gases is an approximation to the more complicated phonon-mediated interaction.

The pairing model of BCS was later shown by R.W Richardson [3] to belong to the set of integrable models, being solvable by a variation of the Bethe ansatz. While Richardson applied the model for studying nuclear physics, the solution method was later used to study the existence of superconductivity in the mesoscopic size regime. The question of the lower size limit for superconductivity was studied by Anderson [4] in 1959 who estimated that superconductivity should begin to vanish for systems of $\sim 10^4$ electrons. Experiments by Black, Ralph and Tinkham (BRT) [5] where Al nanograins of $\sim 10^2$ electrons were shown to exhibit superconducting properties challenged these results though, and various theorists sought to explain the physics of mesoscopic superconductors. A number of approaches were tried, until theorists became aware that the models considered were exactly solvable with

the Richardson approach. Using this method, the energy spectra of mesoscopic superconductors were able to be analysed and the vanishing of superconductivity was able to be studied [6]. Parity, in the sense of an odd/even number of electrons, was demonstrated to have significant importance to the vanishing of superconductivity both experimentally and theoretically. This fact will also be showcased in section 4.1 of this thesis.

1.3 Trapped atoms

Another setting to which the Richardson model can be applied to is that of ultracold atomic gases. Such systems of electrically neutral atoms are expected to interact at lowest order with a contact interaction term as defined (2.1). Recent experiments by Bayha *et al.* [7] have been able to measure the excitation spectrum of small collections of ^{6}Li atoms. In the experiments, the lithium atoms are trapped by an optical tweezer, modelled as a slightly anisotropic two-dimensional harmonic oscillator. At the low temperature regime the experiments study, the interaction of such a system with its surroundings can essentially be neglected. Trapped systems of $M = 3$ and $M = 6$ pairs displayed experimentally a previously theorised precursor to the quantum phase transition observed in the many-body limit as a closing of the excitation energy gap [8]. The experimental results of Bayha *et al.* were confirmed in simulation through numerical diagonalisation of the contact interaction Hamiltonian, with results predicting well the experimentally measured excitation spectrum. Due to computational limits, such diagonalisation techniques are not able to resolve more than 6 interacting particles.

In this thesis, the Richardson model has been applied to produce excitation spectra of harmonically trapped atoms. The main benefit of using the Richardson model compared to exact diagonalisation is the vast lowering of the computational cost which allows for the possibility of studying larger systems numerically. As one of the purposes of the experiments is to study the transition to the thermodynamic limit, being able to simulate larger systems is of great theoretical interest.

The possible anisotropy of the trap will introduce a fine splitting of the degenerate single particle levels. This is discussed further in section 2.5.2. Numerical results are used to motivate that a slightly anisotropic single-particle spectrum leads to the same physical phenomena as the more idealised isotropic single particle spectra. Although there are in principle no problems handling the anisotropy in a Richardson model, the main results of this thesis have been obtained with isotropic spectra.

2

Theory

2.1 From contact to pairing interactions

The interaction between N bosonic neutral particles in D dimensions can be modelled quantum mechanically by adding a contact interaction term

$$H_{\text{int}} = -g \sum_{\substack{i,j=1 \\ i \neq j}}^{N} \delta^D \left(\mathbf{r}_i - \mathbf{r}_j \right) \tag{2.1}$$

to the free particle Hamiltonian (1.3). Here $\mathbf{r}_i$ is the position vector of particle i in the Hamiltonian of the theory. This section will explore how the contact interaction term can be reduced to a pairing interaction, first for the bosonic case and then modified for the fermionic case. Consider this interaction operating on a general two particle second quantised state

$$|\mathbf{k}_1, s_1, \mathbf{k}_2, s_2\rangle = a^\dagger_{\mathbf{k}_1 s_1} a^\dagger_{\mathbf{k}_2 s_2} |0\rangle \tag{2.2}$$

where $\mathbf{k}_i$ denote momenta and s_i index the spin states. Since the particles are bosons, the ladder operators $a_{\mathbf{k}s}$ and $a^\dagger_{\mathbf{k}'s'}$ will have canonical commutation relations, unlike the fermionic case where they would be canonical anticommutation relations. In general a spin-independent two particle operator like (2.1) can be written in second quantised formalism with the spin quantum numbers supressed as

$$\hat{H}_{\text{int}} = \sum_{\substack{\mathbf{k}_1, \mathbf{k}_2 \\ \mathbf{k'}_1, \mathbf{k'}_2}} \sum_{\substack{s_1, s_2 \\ s'_1, s'_2}} \langle \mathbf{k}_1, \mathbf{k}_2 | H_{\text{int}} | \mathbf{k'}_1, \mathbf{k'}_2 \rangle \, a^\dagger_{\mathbf{k}_1 s_1} a^\dagger_{\mathbf{k}_2 s_2} a_{\mathbf{k'}_2 s'_2} a_{\mathbf{k'}_1 s'_1}. \tag{2.3}$$

The interaction Hamiltonian matrix element can now be expanded by inserting identities

$$\begin{aligned} \langle \mathbf{k}_1, \mathbf{k}_2 | H_{\text{int}} | \mathbf{k'}_1, \mathbf{k'}_2 \rangle = \int d^D r_1 \int d^D r_2 \int d^D r'_1 \int d^D r'_2 \, \langle \mathbf{k}_1, \mathbf{k}_2 | \mathbf{r}_1, \mathbf{r_2} \rangle \\ \times \langle \mathbf{r_1}, \mathbf{r}_2 | H_{\text{int}} | \mathbf{r}'_1, \mathbf{r}'_2 \rangle \, \langle \mathbf{r}'_1, \mathbf{r}'_2 | \mathbf{k}'_1, \mathbf{k}'_2 \rangle \, . \end{aligned} \tag{2.4}$$

In position basis, the interaction Hamiltonian is exactly (2.1), giving

$$\begin{aligned} \langle \mathbf{r}_1, \mathbf{r}_2 | H_{\text{int}} | \mathbf{r}'_1, \mathbf{r}'_2 \rangle &= -\, g \, \langle \mathbf{r}_1, \mathbf{r}_2 | \mathbf{r}'_1, \mathbf{r}'_2 \rangle \, \delta^D (\mathbf{r}'_1 - \mathbf{r}'_2) \\ &= -\, g \delta^D (\mathbf{r}_1 - \mathbf{r}'_1) \delta^D (\mathbf{r}_2 - \mathbf{r}'_2) \delta^D (\mathbf{r}'_1 - \mathbf{r}'_2) \end{aligned} \tag{2.5}$$

which yields

$$\begin{aligned}\langle \mathbf{k}_1, \mathbf{k}_2 | H_{\text{int}} | \mathbf{k'}_1, \mathbf{k'}_2 \rangle &= -g \int d^D r_1 \int d^D r_2 \int d^D r'_1 \int d^D r'_2 \, \langle \mathbf{k}_1, \mathbf{k}_2 | \mathbf{r}_1, \mathbf{r}_2 \rangle \, \langle \mathbf{r}'_1, \mathbf{r}'_2 | \mathbf{k}'_1, \mathbf{k}'_2 \rangle \\ &\quad \times \delta^D(\mathbf{r}_1 - \mathbf{r}'_1) \delta^D(\mathbf{r}_2 - \mathbf{r}'_2) \delta^D(\mathbf{r}'_1 - \mathbf{r}'_2) \\ &= -g \int d^D r_1 \int d^D r_2 \, \langle \mathbf{k}_1, \mathbf{k}_2 | \mathbf{r}_1, \mathbf{r}_2 \rangle \, \langle \mathbf{r}_1, \mathbf{r}_2 | \mathbf{k}'_1, \mathbf{k}'_2 \rangle \, \delta(\mathbf{r}_1 - \mathbf{r}_2) \\ &= -g \int d^D r \, \langle \mathbf{k}_1, \mathbf{k}_2 | \mathbf{r}, \mathbf{r} \rangle \, \langle \mathbf{r}, \mathbf{r} | \mathbf{k}'_1, \mathbf{k}'_2 \rangle \\ &= -g \delta^D(\mathbf{k}'_1 + \mathbf{k}'_2 - \mathbf{k}_1 - \mathbf{k}_2),\end{aligned} \tag{2.6}$$

constraining the momentum to be conserved. Inserting this into equation (2.3), one has

$$\hat{H}_{\text{int}} = -g \sum_{\mathbf{k}_1, \mathbf{k}_2, \mathbf{k}'_1} \sum_{\substack{s_1, s_2 \\ s'_1, s'_2}} a^\dagger_{\mathbf{k}_1 s_1} a^\dagger_{\mathbf{k}_2 s_2} a_{-(\mathbf{k}_1 + \mathbf{k}_2 - \mathbf{k}'_1) s'_2} a_{-\mathbf{k}'_1 s'_1}. \tag{2.7}$$

At this point, the interaction is further simplified by assuming that the only the pairs with zero net momentum are relevant for the interaction, implying that $\mathbf{k}_1 + \mathbf{k}_2 = 0$ and removing a summation. In general it is possible to include pairs with net momentum, some effects of which are discussed in section VII of [9]. Under the zero net momentum approximation, the interaction term is then

$$\hat{H}_{\text{int}} = -g \sum_{\mathbf{k}_1, \mathbf{k}_2} \sum_{\substack{s_1, s_2 \\ s'_1, s'_2}} a^\dagger_{\mathbf{k}_1 s_1} a^\dagger_{-\mathbf{k}_1 s_2} a_{-\mathbf{k}_2 s'_2} a_{\mathbf{k}_2 s'_1}. \tag{2.8}$$

For the bosonic case, there is no requirement on the spin of the particles and all of the terms in the spin summation will contribute to the interaction. If the particles are fermions, then the Pauli principle will require that particles have different spin, such that $s_1 \neq s_2$ and $s'_1 \neq s'_2$. For spin 1/2, there are for example 4 such combinations of spin possible. These can be summarised by writing the interaction using the notation of time reversed states created by $a^\dagger_{\mathbf{k}}$ and $a^\dagger_{\bar{\mathbf{k}}}$, with implied opposite spin. The final expression for the interaction Hamiltonian will thus be

$$\hat{H}_{\text{int}} = -g \sum_{\mathbf{k}_1, \mathbf{k}_2} a^\dagger_{\mathbf{k}_1} a^\dagger_{\bar{\mathbf{k}}_1} a_{\bar{\mathbf{k}}_2} a_{\mathbf{k}_2}. \tag{2.9}$$

It has thus been shown that the contact interaction can be reduced to a pairing interaction between time reversed states in second quantised formalism.

2.2 Macroscopic theory of superconductivity

The physics of superconductivity is as previously discussed usually modelled by the pairing Hamiltonian

$$H = \sum_{\mathbf{k}} \varepsilon_{\mathbf{k}} \left(a^\dagger_{\mathbf{k}} a_{\mathbf{k}} + a^\dagger_{\bar{\mathbf{k}}} a_{\bar{\mathbf{k}}} \right) - g \sum_{\mathbf{k}_1, \mathbf{k}_2} a^\dagger_{\mathbf{k}_1} a^\dagger_{\bar{\mathbf{k}}_1} a_{\bar{\mathbf{k}}_2} a_{\mathbf{k}_2} \tag{2.10}$$

studied by BCS [1] in their microscopic theory of superconductivity and described previously in section 1.2. The Hamiltonian (2.10) describes a fermionic field with

energy spectrum $\varepsilon_{\mathbf{k}}$ with a pair interaction with strength characterised by the coupling constant g. The creation operators $a^\dagger_{\mathbf{k}}$ and $a^\dagger_{\bar{\mathbf{k}}}$ create mutually time-reversed states of momentum $\mathbf{k}$ and $-\mathbf{k}$ respectively with opposite spin. Following the procedure of [10] and [11], the theory of superconductivity for macroscopic systems will now be reviewed. To obtain the energy spectrum of the theory, the first step is to couple H to a grand canonical ensemble, modifying the Hamiltonian to

$$H = \sum_{\mathbf{k}} (\varepsilon_{\mathbf{k}} - \mu) \left(a^\dagger_{\mathbf{k}} a_{\mathbf{k}} + a^\dagger_{\bar{\mathbf{k}}} a_{\bar{\mathbf{k}}} \right) - g \sum_{\mathbf{k}_1, \mathbf{k}_2} a^\dagger_{\mathbf{k}_1} a^\dagger_{\bar{\mathbf{k}}_2} a_{\bar{\mathbf{k}}_2} a_{\mathbf{k}_2} \tag{2.11}$$

where μ is the chemical potential for adding a particle to the system, equal to the Fermi energy at zero temperature. For future convenience, define $\eta_{\mathbf{k}} = \varepsilon_{\mathbf{k}} - \mu$. The Bogoliubov transformation can then be introduced as the transformation

$$\begin{aligned} a_{\mathbf{k}} =& u_{\mathbf{k}} \alpha_{\mathbf{k}} + v^*_{\mathbf{k}} \beta^\dagger_{\mathbf{k}} \\ a^\dagger_{\bar{\mathbf{k}}} =& - v_{\mathbf{k}} \alpha_{\mathbf{k}} + u^*_{\mathbf{k}} \beta^\dagger_{\mathbf{k}} \end{aligned} \tag{2.12}$$

where $u_{\mathbf{k}}$ and $v_{\mathbf{k}}$ are real functions of $\mathbf{k}$. Note that the introduced quasiparticle operators are required to obey the same fermionic anticommutation relations as the original operators. This places the condition on $u_{\mathbf{k}}$ and $v_{\mathbf{k}}$ that

$$1 = \{a_{\mathbf{k}+}, a^\dagger_{\mathbf{k}+}\} = u_{\mathbf{k}} v_{\mathbf{k}} \{\alpha_{\mathbf{k}}, \beta_{\mathbf{k}}\} + u^2_{\mathbf{k}} \{\alpha_{\mathbf{k}}, \alpha^\dagger_{\mathbf{k}}\} + v^2_{\mathbf{k}} \{\beta^\dagger_{\mathbf{k}}, \beta_{\mathbf{k}}\} + u_{\mathbf{k}} v_{\mathbf{k}} \{\alpha^\dagger_{\mathbf{k}}, \beta^\dagger_{\mathbf{k}}\} \tag{2.13}$$

with the implication that $u^2_{\mathbf{k}} + v^2_{\mathbf{k}} = 1$.

At this point, the quasiparticle number operators averaged over the grand canonical ensemble

$$n_{\mathbf{k}\alpha} = \left\langle \alpha^\dagger_{\mathbf{k}} \alpha_{\mathbf{k}} \right\rangle \qquad n_{\mathbf{k}\beta} = \left\langle \beta^\dagger_{\mathbf{k}} \beta_{\mathbf{k}} \right\rangle \tag{2.14}$$

can also be introduced. The next step is to express the Hamiltonian in the transformed basis. As a start, the number operator for the two mutually time-reversed particle states of momenta $\mathbf{k}$ and $\bar{\mathbf{k}}$ are evaluated in the new basis. They are

$$\begin{aligned} a^\dagger_{\mathbf{k}} a_{\mathbf{k}} =& (v_{\mathbf{k}} \beta_{\mathbf{k}} + u_{\mathbf{k}} \alpha^\dagger_{\mathbf{k}})(u_{\mathbf{k}} \alpha_{\mathbf{k}} + v_{\mathbf{k}} \beta^\dagger_{\mathbf{k}}) \\ =& u^2_{\mathbf{k}} \alpha^\dagger_{\mathbf{k}} \alpha_{\mathbf{k}} + u_{\mathbf{k}} v_{\mathbf{k}} \beta_{\mathbf{k}} \alpha_{\mathbf{k}} + u_{\mathbf{k}} v_{\mathbf{k}} \alpha^\dagger_{\mathbf{k}} \beta^\dagger_{\mathbf{k}} + v^2_{\mathbf{k}} \beta_{\mathbf{k}} \beta^\dagger_{\mathbf{k}} \\ a^\dagger_{\bar{\mathbf{k}}} a_{\bar{\mathbf{k}}} =& (-v_{\mathbf{k}} \alpha_{\mathbf{k}} + u_{\mathbf{k}} \beta^\dagger_{\mathbf{k}})(-v_{\mathbf{k}} \alpha^\dagger_{\mathbf{k}} + u_{\mathbf{k}} \beta_{\mathbf{k}}) \\ =& v^2_{\mathbf{k}} \alpha_{\mathbf{k}} \alpha^\dagger_{\mathbf{k}} - u_{\mathbf{k}} v_{\mathbf{k}} \alpha_{\mathbf{k}} \beta_{\mathbf{k}} - u_{\mathbf{k}} v_{\mathbf{k}} \beta^\dagger_{\mathbf{k}} \alpha^\dagger_{\mathbf{k}} + u^2_{\mathbf{k}} \beta^\dagger_{\mathbf{k}} \beta_{\mathbf{k}}. \end{aligned} \tag{2.15}$$

In the new Bogoliubov basis, the non-interacting term $F_{\mathbf{k}}$ is therefore

$$\begin{aligned} F_{\mathbf{k}} \equiv& a^\dagger_{\mathbf{k}} a_{\mathbf{k}} + a^\dagger_{\bar{\mathbf{k}}} a_{\bar{\mathbf{k}}} = 2v^2_{\mathbf{k}} + \left(u^2_{\mathbf{k}} - v^2_{\mathbf{k}} \right) \left(\alpha^\dagger_{\mathbf{k}} \alpha_{\mathbf{k}} + \beta^\dagger_{\mathbf{k}} \beta_{\mathbf{k}} \right) \\ &+ u_{\mathbf{k}} v_{\mathbf{k}} \left(\beta_{\mathbf{k}} \alpha_{\mathbf{k}} - \alpha_{\mathbf{k}} \beta_{\mathbf{k}} \right) + u_{\mathbf{k}} v_{\mathbf{k}} \left(\alpha^\dagger_{\mathbf{k}} \beta^\dagger_{\mathbf{k}} - \beta^\dagger_{\mathbf{k}} \alpha^\dagger_{\mathbf{k}} \right). \end{aligned} \tag{2.16}$$

The second term of the Hamiltonian (2.11) can be simplified by introducing the pair operator

$$D_{\mathbf{k}} \equiv a_{\bar{\mathbf{k}}} a_{\mathbf{k}} = u^2_{\mathbf{k}} \beta_{\mathbf{k}} \alpha_{\mathbf{k}} + u_{\mathbf{k}} v_{\mathbf{k}} \left(1 - \alpha^\dagger_{\mathbf{k}} \alpha_{\mathbf{k}} - \beta^\dagger_{\mathbf{k}} \beta_{\mathbf{k}} \right) - v^2_{\mathbf{k}} \alpha^\dagger_{\mathbf{k}} \beta^\dagger_{\mathbf{k}} \tag{2.17}$$

so that the Hamiltonian can be written

$$H' = \sum_{\mathbf{k}} \eta_{\mathbf{k}} F_{\mathbf{k}} - g \sum_{\mathbf{k}_1} \sum_{\mathbf{k}_2} D^\dagger_{\mathbf{k}_1} D_{\mathbf{k}_2}. \tag{2.18}$$

The average energy of the system may now be calculated by averaging over the grand canonical ensemble

$$E = \langle H' \rangle = \sum_{\mathbf{k}} \eta_{\mathbf{k}} \langle F_{\mathbf{k}} \rangle - g \sum_{\mathbf{k}_1} \sum_{\mathbf{k}_2} \left\langle D^\dagger_{\mathbf{k}_1} D_{\mathbf{k}_2} \right\rangle. \tag{2.19}$$

The first term can easily be calculated by utilising the fact that the only combinations of quasiparticle operators with non-zero ensemble average are those in (2.14). Thus, it evaluates to

$$\langle F_{\mathbf{k}} \rangle = 2v^2_{\mathbf{k}} + (u^2_{\mathbf{k}} - v^2_{\mathbf{k}}) (n_{\mathbf{k}\alpha} + n_{\mathbf{k}\beta}). \tag{2.20}$$

To proceed further, the interaction term $D^\dagger_{\mathbf{k}_1} D_{\mathbf{k}_2}$ is rewritten by expressing all of the operators as an average and a small fluctuation around this average, giving

$$\beta_{\mathbf{k}} \alpha_{\mathbf{k}} = \langle \beta_{\mathbf{k}} \alpha_{\mathbf{k}} \rangle + (\beta_{\mathbf{k}} \alpha_{\mathbf{k}} - \langle \beta_{\mathbf{k}} \alpha_{\mathbf{k}} \rangle) \tag{2.21}$$

for $\beta_{\mathbf{k}} \alpha_{\mathbf{k}}$ and similar expressions for the other operator combinations. By neglecting terms quadratic in the fluctuations and remembering once again that the only combinations of quasiparticle operators with non-zero ensemble average are those in (2.14), the interaction term is approximated as

$$\begin{aligned}
D^\dagger_{\mathbf{k}_1} D_{\mathbf{k}_2} \approx & u_{\mathbf{k}_1} u_{\mathbf{k}_2} v_{\mathbf{k}_1} v_{\mathbf{k}_2} \left(1 - \left\langle \alpha_{\mathbf{k}_1} \alpha^\dagger_{\mathbf{k}_1} \right\rangle - \left\langle \beta_{\mathbf{k}_1} \beta^\dagger_{\mathbf{k}_1} \right\rangle\right) \left(1 - \left\langle \alpha^\dagger_{\mathbf{k}_2} \alpha_{\mathbf{k}_2} \right\rangle - \left\langle \beta^\dagger_{\mathbf{k}_2} \beta_{\mathbf{k}_2} \right\rangle\right) \\
& + u_{\mathbf{k}_1} v_{\mathbf{k}_1} \left(u^2_{\mathbf{k}_2} \beta_{\mathbf{k}_2} \alpha_{\mathbf{k}_2} - v^2_{\mathbf{k}_2} \alpha^\dagger_{\mathbf{k}_2} \beta^\dagger_{\mathbf{k}_2}\right) \left(1 - \left\langle \alpha_{\mathbf{k}_1} \alpha^\dagger_{\mathbf{k}_1} \right\rangle - \left\langle \beta_{\mathbf{k}_1} \beta^\dagger_{\mathbf{k}_1} \right\rangle\right) \\
& + \left(u^2_{\mathbf{k}_1} \alpha^\dagger_{\mathbf{k}_1} \beta^\dagger_{\mathbf{k}_1} - v^2_{\mathbf{k}_1} \beta_{\mathbf{k}_1} \alpha_{\mathbf{k}_1}\right) u_{\mathbf{k}_1} v_{\mathbf{k}_1} \left(1 - \left\langle \alpha^\dagger_{\mathbf{k}_2} \alpha_{\mathbf{k}_2} \right\rangle - \left\langle \beta^\dagger_{\mathbf{k}_2} \beta_{\mathbf{k}_2} \right\rangle\right) \\
& + u_{\mathbf{k}_1} u_{\mathbf{k}_2} v_{\mathbf{k}_1} v_{\mathbf{k}_2} \left(1 - \left\langle \alpha_{\mathbf{k}_1} \alpha^\dagger_{\mathbf{k}_1} \right\rangle - \left\langle \beta_{\mathbf{k}_1} \beta^\dagger_{\mathbf{k}_1} \right\rangle\right) \\
& \times \left(1 - \alpha^\dagger_{\mathbf{k}_2} \alpha_{\mathbf{k}_2} + \left\langle \alpha^\dagger_{\mathbf{k}_2} \alpha_{\mathbf{k}_2} \right\rangle - \beta^\dagger_{\mathbf{k}_2} \beta_{\mathbf{k}_2} + \left\langle \beta^\dagger_{\mathbf{k}_2} \beta_{\mathbf{k}_2} \right\rangle\right) \\
& + u_{\mathbf{k}_1} u_{\mathbf{k}_2} v_{\mathbf{k}_1} v_{\mathbf{k}_2} \left(1 - \alpha_{\mathbf{k}_1} \alpha^\dagger_{\mathbf{k}_1} + \left\langle \alpha_{\mathbf{k}_1} \alpha^\dagger_{\mathbf{k}_1} \right\rangle - \beta_{\mathbf{k}_1} \beta^\dagger_{\mathbf{k}_1} + \left\langle \beta_{\mathbf{k}_1} \beta^\dagger_{\mathbf{k}_1} \right\rangle\right) \\
& \times \left(1 - \left\langle \alpha^\dagger_{\mathbf{k}_2} \alpha_{\mathbf{k}_2} \right\rangle - \left\langle \beta^\dagger_{\mathbf{k}_2} \beta_{\mathbf{k}_2} \right\rangle\right)
\end{aligned} \tag{2.22}$$

which is essentially equivalent to using the mean-field theory approximation. By now taking the average of the interaction term, one has that

$$\left\langle D^\dagger_{\mathbf{k}_1} D_{\mathbf{k}_2} \right\rangle = u_{\mathbf{k}_1} u_{\mathbf{k}_2} v_{\mathbf{k}_1} v_{\mathbf{k}_2} (1 - n_{\mathbf{k}_1\alpha} - n_{\mathbf{k}_1\beta}) (1 - n_{\mathbf{k}_2\alpha} - n_{\mathbf{k}_2\beta}) \tag{2.23}$$

from which one can conclude that $\left\langle D^\dagger_{\mathbf{k}_1} D_{\mathbf{k}_2} \right\rangle = \langle D^\dagger_{\mathbf{k}_1} \rangle \langle D_{\mathbf{k}_2} \rangle$ which implies that

$$\langle D_{\mathbf{k}} \rangle = u_{\mathbf{k}} v_{\mathbf{k}} (1 - n_{\mathbf{k}\alpha} - n_{\mathbf{k}\beta}). \tag{2.24}$$

The energy gap parameter Δ is next introduced as the sum of the averaged values of $D_{\mathbf{k}}$

$$\Delta = g \sum_{\mathbf{k}} \langle D_{\mathbf{k}} \rangle \tag{2.25}$$

so that the average energy is

$$E = \sum_{\mathbf{k}} \eta_{\mathbf{k}} \left[2v_{\mathbf{k}}^2 + (u_{\mathbf{k}}^2 - v_{\mathbf{k}}^2)(n_{\mathbf{k}\alpha} + n_{\mathbf{k}\beta}) \right] - \frac{1}{g}\Delta^2. \tag{2.26}$$

From the principle of maximum entropy of thermodynamics one has that at thermodynamic equilibrium the energy should be minimised at constant entropy. Since the entropy of the system is defined

$$\begin{aligned} S = -\sum_{\mathbf{k}} [& n_{\mathbf{k}\alpha} \log(n_{\mathbf{k}\alpha}) + n_{\mathbf{k}\beta} \log(n_{\mathbf{k}\beta}) \\ & + (1 - n_{\mathbf{k}\alpha}) \log(1 - n_{\mathbf{k}\alpha}) + (1 - n_{\mathbf{k}\beta}) \log(1 - n_{\mathbf{k}\beta})] \end{aligned} \tag{2.27}$$

and only depends on the occupation numbers $n_{\mathbf{k}\alpha}$ and $n_{\mathbf{k}\beta}$, it follows that minimising the energy with respect to fixed entropy implies minimising the energy with respect to fixed occupation numbers. Keeping in mind that the variables $u_{\mathbf{k}}$ and $v_{\mathbf{k}}$ are constrained by $u_{\mathbf{k}}^2 + v_{\mathbf{k}}^2 = 1$, it suffices to minimise in one of these variables. For convenience, define the total level occupancy $N_{\mathbf{k}} = n_{\mathbf{k}\alpha} + n_{\mathbf{k}\beta}$. Deriving with respect to $u_{\mathbf{k}}$, one has

$$\frac{\partial E}{\partial u_{\mathbf{k}}} = 4\eta_{\mathbf{k}} \left[N_{\mathbf{k}} - 1 \right] u_{\mathbf{k}} - 2 \left[1 - N_{\mathbf{k}} \right] \Delta \frac{1 - 2u_{\mathbf{k}}^2}{\sqrt{1 - u_{\mathbf{k}}^2}} = 0. \tag{2.28}$$

After some algebra, one finds the equation

$$2\eta_{\mathbf{k}} u_{\mathbf{k}} v_{\mathbf{k}} = \Delta \left(u_{\mathbf{k}}^2 - v_{\mathbf{k}}^2 \right) \tag{2.29}$$

which has solutions

$$\begin{aligned} u_{\mathbf{k}}^2 &= \frac{1}{2} \left(1 + \frac{\eta_{\mathbf{k}}}{\sqrt{\Delta^2 + \eta_{\mathbf{k}}^2}} \right) \\ v_{\mathbf{k}}^2 &= \frac{1}{2} \left(1 - \frac{\eta_{\mathbf{k}}}{\sqrt{\Delta^2 + \eta_{\mathbf{k}}^2}} \right). \end{aligned} \tag{2.30}$$

The energy for creating an excitation of momentum $\mathbf{k}$ in the interacting system can then be found by varying the total energy with respect to the quasiparticle occupation numbers $n_{\mathbf{k}\alpha}$ and $n_{\mathbf{k}\beta}$. One has that

$$\begin{aligned} \epsilon_{\mathbf{k}} &= \frac{\partial E}{\partial n_{\mathbf{k}\alpha}} = \frac{\partial E}{\partial n_{\mathbf{k}\beta}} = \eta_{\mathbf{k}} \left(u_{\mathbf{k}}^2 - v_{\mathbf{k}}^2 \right) + 2\Delta u_{\mathbf{k}} v_{\mathbf{k}} \\ &= \frac{\eta_{\mathbf{k}}^2}{\sqrt{\Delta^2 + \eta_{\mathbf{k}}^2}} + \frac{\Delta^2}{\sqrt{\Delta^2 + \eta_{\mathbf{k}}^2}} = \sqrt{\Delta^2 + \eta_{\mathbf{k}}^2}. \end{aligned} \tag{2.31}$$

This energy spectrum is characteristic of a superconductor. A sketch of the spectrum is shown in figure 2.1, the superconductor being dash-dotted and the non-interacting system being filled.

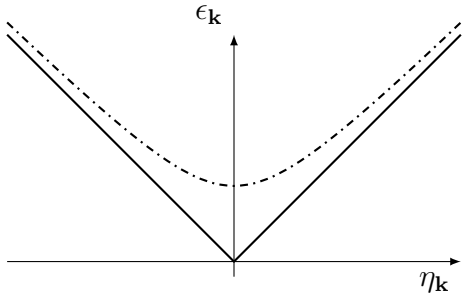

Figure 2.1: The modified energy spectrum resulting from the gap Δ in a superconductor.

If Δ is much larger than the single particle energies, then the spectrum is approximately continuous after an initial energy gap. The energy gap Δ is mesurable in various experiments, an early example of which is by Giaever [12]. One can go further and use the solutions (2.30) in the definition of Δ to write the gap equation

$$\Delta = g \sum_{\mathbf{k}} \frac{1}{2}(1 - n_{\mathbf{k}\alpha} - n_{\mathbf{k}\beta}) \sqrt{1 - \frac{\eta_{\mathbf{k}}^2}{\Delta^2 + \eta_{\mathbf{k}^2}}} \tag{2.32}$$

which can be further simplified to

$$\frac{1}{g} = \sum_{\mathbf{k}} \frac{1 - n_{\mathbf{k}\alpha} - n_{\mathbf{k}\beta}}{2\epsilon_{\mathbf{k}}}. \tag{2.33}$$

Since the quasiparticles are fermions, they follow Fermi-Dirac statistics and have

$$n_{\mathbf{k}\alpha} = n_{\mathbf{k}\beta} = \frac{1}{e^{\beta\epsilon_{\mathbf{k}}} + 1} \tag{2.34}$$

which gives, taking the zero temperature limit

$$\frac{1}{g} = \sum_{\mathbf{k}} \frac{1}{2\epsilon_{\mathbf{k}}} \frac{e^{\beta\epsilon_{\mathbf{k}}} - 1}{e^{\beta\epsilon_{\mathbf{k}}} + 1} \xrightarrow[\beta\to\infty]{} \sum_{|\mathbf{k}|<k_F} \frac{1}{2\epsilon_{\mathbf{k}}} \tag{2.35}$$

where the fact that at zero temperature states with momentum up to the Fermi momentum are occupied was used. This equation can now be used to relate the interaction strength to the energy gap. While these results have been obtained in a grand canonical ensemble and are thus valid for macroscopic systems, one would expect that this result should be approached by mesoscopic systems as their size is increased.

As a closing remark to this section, BCS used the product

$$|\psi_G\rangle = \prod_{|\mathbf{k}|<k_F} \left(u_{\mathbf{k}}^2 + v_{\mathbf{k}}^2 a_{\mathbf{k}}^\dagger a_{\bar{\mathbf{k}}}^\dagger\right) |0\rangle \tag{2.36}$$

as an ansatz for the ground state $|\psi_G\rangle$ so that $u_{\mathbf{k}}^2$ is interpreted as the probability of the state labelled by $\mathbf{k}$ being empty and $v_{\mathbf{k}}^2$ being the probability of it being occupied by a pair. This provides a physical interpretation of the theory as a condensation of Cooper pairs created by $D_{\mathbf{k}}^\dagger = a_{\mathbf{k}}^\dagger a_{\bar{\mathbf{k}}}^\dagger$. Cooper pairs created by such pair operators will play a central role in the Richardson approach to pairing interactions which will be developed in the following sections.

2.3 Mesoscopic theory of superconductivity

The grand canonical approach used in the BCS theory is valid in the thermodynamic limit of a large number of particles. Motivated by the experiments of BRT [5] where Al nanograins were shown to exhibit superconducting properties, various theorists sought to explain the physics of mesoscopic superconductors. The size of a superconductor can be characterised by the fraction d/Δ where d is the mean level spacing and Δ is the bulk superconducting energy gap introduced in equation (2.25). Essentially, the reason for superconductivity is the existence of a ground state of condensed pairs of the type (2.36).

Starting from the results of BRT, von Delft *et al.* [13] identified the importance of parity for mesoscopic superconductors. Parity in this context reflects an even or odd number of particles. They used a parity projected grand-canonical approach to find that the pairing correlations would vanish abrubtly for a critical mean level spacing d_C. Their means to study the vanishing of the pairing correlations was the condensation energy, defined as

$$E_C(N) = \mathcal{E}_G(N) - \langle F_N | \, H \, | F_N \rangle \tag{2.37}$$

where $|F_N\rangle$ represents an N-particle state in the free theory and $\mathcal{E}_G$ being the ground state energy obtained in the interacting theory. The condensation energy is a measure of the favourability of the system condensing into a paired state and can be studied to see the appearance of superconductivity for increasing system sizes. It was shown that superconductivity would vanish for larger d/Δ for even than for odd grains. The abrubt vanishing of superconductivity was later shown to be an artifact of the grand-canonical approach [14], and thus not physical in the mesoscopic systems. In the BCS theory, the condensation energy can be calculated by recalling equation (2.26) and using that $\Delta = 0$ in the free theory. The BCS condensation energy is thus

$$E_C = -\frac{1}{g}\Delta^2 \tag{2.38}$$

which will later be compared to the results obtained using the models developed here.

Matveev and Larkin [15] continued the analysis of the experiments of BRT, and introduced an additional parity parameter, later known as the Matveev-Larkin parameter

$$\Delta_{ML}(N) = \mathcal{E}_G(N) - \frac{1}{2}\left[\mathcal{E}_G(N+1) + \mathcal{E}_G(N-1)\right] \tag{2.39}$$

where N is an odd integer and denotes the number of particles in the system. The definition states that the Matveev-Larkin parameter is the difference between the energy of the system with an unpaired particle and the mean of the energy of neighbouring fully paired states. Matveev and Larkin found the limiting case in the fluctuation-dominated regime for Δ_{ML} when $d \gg \Delta$

$$\Delta_{ML} = \frac{d}{2\ln\frac{d}{\Delta}} \tag{2.40}$$

by using renormalisation arguments, predicting that the parity effects should be stronger in smaller systems. They also found the $d \ll \Delta$ limit of Δ_{ML} as

$$\Delta_{ML} = \Delta - \frac{d}{2} \tag{2.41}$$

Taken together, these limits imply a minima of the Matveev-Larkin parameter at the energy scale $d \sim \Delta$, at the crossover from the superconducting to the fluctuation-dominated regime.

2.4 The Richardson approach

In the same context of mesoscopic superconductors, it was later realised that the analytical solution to the reduced BCS Hamiltonian developed by Richardson [3] was applicable to mesoscopic superconductors. In this section the Richardson approach will be used to develop a theory for obtaining the energy spectrum of the reduced BCS Hamiltonian in mesoscopic systems. The Hamiltonian (2.10) restricted to one dimension is usually written as

$$H = \sum_{\tau=+,-} \sum_{j=1}^{n} \varepsilon_j a_{j\tau}^\dagger a_{j\tau} - g \sum_{i=1}^{n} \sum_{j=1}^{n} a_{i+}^\dagger a_{i-}^\dagger a_{j-} a_{j+} \tag{2.42}$$

with a spectral cutoff n is used. Here the mutually time-reversed states are indexed by τ and as before the interaction only couples time-reversed paired states.

2.4.1 Formalism and the perturbative case

As a first approximation and a check for the developed theory, perturbation theory will be used to obtain a first-order prediction for the spectrum. It is essential to note that the interaction term of the Hamiltonian (2.42) only couples pairs to one another and that singly occupied states do not participate in the interaction. A Hilbert subspace $\mathcal{U}$ to the full Hilbert space $\mathcal{H}$ of pairs may be defined where the singly occupied levels are excluded, as indicated in figure 2.2. For the perturbative calcuations, the corrections will thus only concern the part of a state in $\mathcal{U}$. Introduce now the pair creation and annihilation operators $b_j^\dagger = a_{j+}^\dagger a_{j-}^\dagger$ and $b_j = a_{j-} a_{j+}$. Depending on what statistics the particles follow, the pair operators will acquire commutation relations accordingly. For fermionic statistics, the non-zero commutators are

$$\begin{aligned}
[b_i, b_j^\dagger] =& [a_{i-}a_{i+}, a_{j+}^\dagger a_{j-}^\dagger] = a_{i-}a_{i+}a_{j+}^\dagger a_{j-}^\dagger - a_{j+}^\dagger a_{j-}^\dagger a_{i-}a_{i+} \\
=& - a_{i-}a_{j+}^\dagger a_{i+}a_{j-}^\dagger + a_{i-}a_{j-}^\dagger \delta_{ij} - a_{j+}^\dagger a_{j-}^\dagger a_{i-}a_{i+} \\
=& a_{j+}^\dagger a_{i-}a_{i+}a_{j-}^\dagger + a_{i-}a_{j-}^\dagger \delta_{ij} - a_{j+}^\dagger a_{j-}^\dagger a_{i-}a_{i+} \\
=& - a_{j+}^\dagger a_{i-}a_{j-}^\dagger a_{i+} + a_{i-}a_{j-}^\dagger \delta_{ij} - a_{j+}^\dagger a_{j-}^\dagger a_{i-}a_{i+} \\
=& a_{j+}^\dagger a_{j-}^\dagger a_{i-}a_{i+} + a_{i-}a_{j-}^\dagger \delta_{ij} - a_{j+}^\dagger a_{i+}\delta_{ij} - a_{j+}^\dagger a_{j-}^\dagger a_{i-}a_{i+} \\
=& \left(1 - a_{j-}^\dagger a_{j-} - a_{j+}^\dagger a_{j+}\right)\delta_{ij}
\end{aligned} \tag{2.43}$$

which are called hard-core boson commutation relations. When one restricts to the Hilbert subspace $\mathcal{U}$, the commutation relations are able to be expressed in the pair operators as

$$[b_i, b_j^\dagger] = \left(1 - 2b_j^\dagger b_j\right) \delta_{ij}. \tag{2.44}$$

For bosons, one has instead

$$[b_i, b_j^\dagger] = \left(1 + a_{j+}^\dagger a_{j+} - a_{j-}^\dagger a_{j-}\right) \delta_{ij} \tag{2.45}$$

which reduces to

$$[b_i, b_j^\dagger] = \delta_{ij} \tag{2.46}$$

on $\mathcal{U}$. As will now be shown, first order perturbation theory yields the same result independently of particle statistics. A general eigenstate of the full Hamiltonian can be written as a tensor product of a state built out of the pair operators in $\mathcal{U}$ and a state built out of the single particle operators in $\mathcal{U}^c = \mathcal{H} \setminus \mathcal{U}$. Figure 2.2 shows an interpertation of this restriction for the harmonic oscillator.

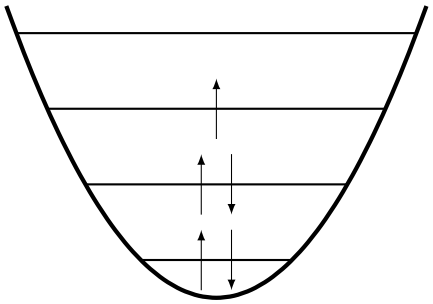

(a) Ground state of the noninteracting fermion system in a harmonic oscillator potential.

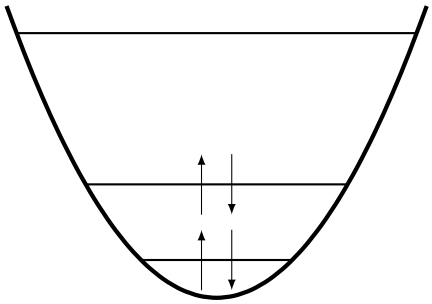

(b) The Hilbert subspace U where the singly occupied levels are blocked.

Figure 2.2: A simple example of the implications of restricting to the subspace U of the Hilbert space.

A general state of L unpaired particles and M pairs of particles can now be written with the pair creation operators as

$$|\Psi\rangle = |\phi\rangle \otimes |\psi\rangle = \prod_{\mu=1}^{L} a_{k_\mu \tau_\mu}^\dagger |0_s\rangle \otimes \prod_{\nu=1}^{M} b_{k_\nu}^\dagger |0_p\rangle . \tag{2.47}$$

Since the interaction term is restricted to $\mathcal{U}$, it suffices to consider only states in $\mathcal{U}$. The Hamiltonian restricted to $\mathcal{U}$, assuming no blocked levels, is

$$H_{\mathcal{U}} = \sum_{i=1}^{n} \sum_{j=1}^{n} \left(2\varepsilon_j \delta_{ij} - g\right) b_i^\dagger b_j \tag{2.48}$$

with the interaction term being

$$H_{\text{int}} = -g \sum_{i=1}^{n} \sum_{j=1}^{n} b_i^\dagger b_j. \tag{2.49}$$

First order perturbation theory now gives

$$\begin{aligned}
\langle\psi|\, H_{\text{int}}\, |\psi\rangle &= -\, g\, \langle\psi| \left[H_{\text{int}}, \prod_{\nu=1}^{M} b_{k_\nu}^\dagger\right] |0\rangle \\
&= -\, g \sum_{i=1}^{n}\sum_{j=1}^{n} \langle\psi|\, b_i^\dagger \left[b_j, \prod_{\nu=1}^{M} b_{k_\nu}^\dagger\right] |0\rangle \\
&= -\, g \sum_{i=1}^{n}\sum_{j=1}^{n} \langle\psi|\, b_i^\dagger \sum_{\nu=1}^{M} \left(\prod_{\mu=1}^{\nu-1} b_{k_\mu}^\dagger\right) \left[b_j, b_{k_\nu}^\dagger\right] \left(\prod_{\eta=\nu+1}^{M} b_{k_\eta}^\dagger\right) |0\rangle \\
&= -\, g \sum_{i=1}^{n}\sum_{j=1}^{n} \langle\psi|\, b_i^\dagger \sum_{\nu=1}^{M} \left(\prod_{\mu=1}^{\nu-1} b_{k_\mu}^\dagger\right) \left(1 - 2b_j^\dagger b_j\right) \delta_{jk_\nu} \left(\prod_{\eta=\nu+1}^{M} b_{k_\eta}^\dagger\right) |0\rangle \\
&= -\, g \sum_{i=1}^{n}\sum_{\nu=1}^{M} \langle\psi|\, b_i^\dagger \left(\prod_{\mu\neq\nu}^{M} b_{k_\nu}^\dagger\right) |0\rangle \\
&= -\, g \sum_{\kappa=1}^{M}\sum_{\nu=1}^{M} \langle 0| \prod_{\iota\neq\kappa}^{M} b_{k_\iota} \prod_{\mu\neq\nu}^{M} b_{k_\nu}^\dagger |0\rangle \\
&= -\, g \sum_{\kappa=1}^{M}\sum_{\nu=1}^{M} \delta_{\kappa\nu} \\
&= -\, gM
\end{aligned} \tag{2.50}$$

as the shift in the total energy by introducing the pair interaction. In this evaluation the useful general commutator identity

$$[\alpha, \prod_{i=1}^{n} \beta_i] = \sum_{i=1}^{n} \left(\prod_{j=1}^{i-1} \beta_j\right) [\alpha, \beta_i] \left(\prod_{k=i+1}^{n} \beta_k\right) \tag{2.51}$$

was utilised, which will also be helpful later. Since $|\psi\rangle$ is an arbitrary state of M pairs, this perturbative result is valid for ground states as well as excited states, independently of particle statistics.

2.4.2 The bosonic case

In the case that the interacting pairs would be true bosons, there is a simple solution to the reduced BCS Hamiltonian (2.42) available. Consider bosonic operators b_j and $b_j^\dagger$ with the bosonic commutation relations (2.46) and Hamiltonian (2.48) with non-degenerate spectrum. In matrix form, the Hamiltonian has elements

$$H_{ij} = (2\varepsilon_j \delta_{ij} - g) b_i^\dagger b_j. \tag{2.52}$$

The aim is to find a transformation that diagonalises this matrix, such that

$$H_{IJ} = E_J \delta_{IJ} B_I^\dagger B_J \tag{2.53}$$

for some new operators $B_J^\dagger$, B_J. The second term in H_{ij} can be written as $-g u_i u_j$ for $u_i = (1, 1, ..., 1)$. The Bunch-Nielsen-Sorensen formula [16] relates the eigenvectors and eigenvalues of the sum of a diagonal matrix and a matrix written as an

outer product to the eigenvectors and eigenvalues of the diagonal matrix. From this formula

$$B_J^\dagger = gC_J \frac{u_i \delta^{ij} b_j^\dagger}{2\varepsilon_j - E_J} = gC_J \sum_{j=1}^{n} \frac{b_j^\dagger}{2\varepsilon_j - E_J} \tag{2.54}$$

where N_J is a normalisation constant, which can be found by requiring that $[B_I, B_J^\dagger] = \delta_{IJ}$, giving

$$[B_I, B_J^\dagger] = C_I C_J \sum_{i=1}^{n}\sum_{j=1}^{n} \frac{g^2[b_i, b_j^\dagger]}{(2\varepsilon_i - E_I)(2\varepsilon_j - E_J)} = C_I C_J \sum_{j=1}^{n} \frac{g^2}{(2\varepsilon_j - E_I)(2\varepsilon_j - E_J)} = \delta_{IJ}. \tag{2.55}$$

This requires in turn that

$$C_I C_J = \left(\sum_{j=1}^{n} \frac{g^2}{(2\varepsilon_i - E_J)^2} \right)^{-1} \delta_{IJ}. \tag{2.56}$$

The energies E_J can then be found by solving the eigenvalue equation

$$\det\left(H_{ij} - E_J \delta_{ij}\right) = \det\left((2\varepsilon_j - E_J)\delta_{ij} - g u_i u_j\right) = 0. \tag{2.57}$$

By the matrix determinant lemma

$$\begin{aligned} 0 =& \det\left((2\varepsilon_j - E_J)\delta_{ij} - g u_i u_j\right) = \left[1 - g u_i \frac{\delta^{ij}}{2\varepsilon_j - E_J} u_j\right] \det\left((2\varepsilon_j - E_J)\delta_{ij}\right) \\ =& \left(1 - g \sum_{j=1}^{n} \frac{1}{2\varepsilon_j - E_J}\right) \prod_{j=1}^{n} (2\varepsilon_j - E_J). \end{aligned} \tag{2.58}$$

There are two cases to this equation. The first case is that $2\varepsilon_j = E_J$ for some j. This is the only solution available for $g = 0$. The second case is that $2\varepsilon_j \neq E_J$ for all j, which implies that the product may be divided out and the bosonic Richardson equations

$$\frac{1}{g} - \sum_{j=1}^{n} \frac{1}{2\varepsilon_j - E_J} = 0 \tag{2.59}$$

valid for $g \neq 0$ may be obtained. Note that this means that both attractive and repulsive interaction can be studied with the Richardson approach. States in the interacting theory are then assembled from the transformed operators $B_J^\dagger$ such that a general M pair state has the form

$$|\psi\rangle = \prod_{\nu=1}^{M} B_{J_\nu}^\dagger |0\rangle \tag{2.60}$$

where J_ν are ordered after ascending Richardson energies.

2.4.3 The fermionic case

In the fermionic case, one needs to take into account the hard-core boson commutation relations (2.44). The idea in this case is to try the same ansatz (2.60) as in

the bosonic case and see what complications arise. Using the same definition (2.54) as earlier for $B_J^\dagger$ and

$$B_0^\dagger = \sum_{j=1}^{n} b_j^\dagger \tag{2.61}$$

the Hamiltonian (2.48) restricted to $\mathcal{U}$ can also be written

$$H_{\mathcal{U}} = \sum_{j=1}^{n} 2\varepsilon_j b_j^\dagger b_j - g B_0^\dagger B_0. \tag{2.62}$$

Equations for E_J are then derived by requiring that $H_{\mathcal{U}} |\psi\rangle = \mathcal{E} |\psi\rangle$ for some state $|\psi\rangle$ comprised of M pairs, assembled as in equation (2.60). Here $\mathcal{E}$ denotes an unknown energy eigenvalue, related to the total energy by $E = E_\mathrm{s} + \mathcal{E}$ where E_s is the energy of the unpaired particles. Such equations will be found in section 2.4.5 after the generalisation to degenerate systems has been made.

2.4.4 The relation between multidimensionality and degeneracy

In this section, the background will be set for the Richardson method to be expanded to include multi-dimensional fields, where the spectrum is characterised by multiple quantum numbers. In general, this allows for states to be degenerate in energy. The two-dimensional harmonic oscillator is an example of this, with the degenerate levels illustrated in figure 2.3. This means that in general the M-pair ground state will be degenerate. States with completely filled levels, are called closed-shell states. Such states have the useful property that their ground state is unique.

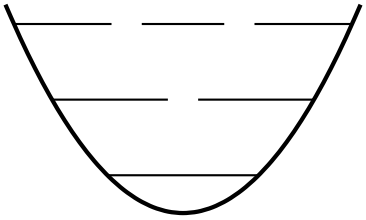

Figure 2.3: The figure illustrates the degeneracy of the two dimensional harmonic oscillator.

If one is able to express the multi-dimensional spectrum of the theory with one quantum number and a degeneration number, the multi-dimensional spectrum could effectively be reduced to a one-dimensional spectrum. Consider as an example of this again the two dimensional harmonic oscillator with an equidistant spectrum $\varepsilon_{ij} = \hbar\omega(i + j + 1)$. The matrix generated by ε_{ij} at cutoff index n will have the structure

$$\varepsilon_{ij} = \hbar\omega \begin{pmatrix} 1 & 2 & ... & ... & n \\ 2 & 3 & ... & n & 0 \\ 3 & ... & n & 0 & 0 \\ ... & ... & ... & ... & ... \\ n & 0 & ... & ... & 0 \end{pmatrix} \tag{2.63}$$

By inspection, one sees that the spectrum can be equivalently enumerated by a single number j' with the energy being $\varepsilon_{j'} = \hbar\omega(j'+1)$ and a degeneracy number $\Omega_{j'} = j'+1$. If one allows levels to be singly occupied and thus blocked from participating the total degeneracy of energy level $\varepsilon_{j'}$ is $\Omega_{j'} = j'+1-s_{j'}$ with $s_{j'} = 0, 1, ..., j'+1$ denoting the number of blocked levels.

When including splitting pairs into unpaired fermions, there are additional first excitations compared to exciting a pair to the next level. It should also be noted that the degeneration introduces additional first excitations compared to the non-degenerate case. The degeneration of all of these is expected to be lifted when the interaction is turned on. While these states are not possible to excite through pairing interactions, it is expected that next order interactions should be able to excite them and they are thus relevant for fitting spectra to experimental data. The figure 2.4 illustrate the additional first excited states for the two-dimensional harmonic oscillator, which in addition to exciting a single pair comprise the spectrum of first excitations.

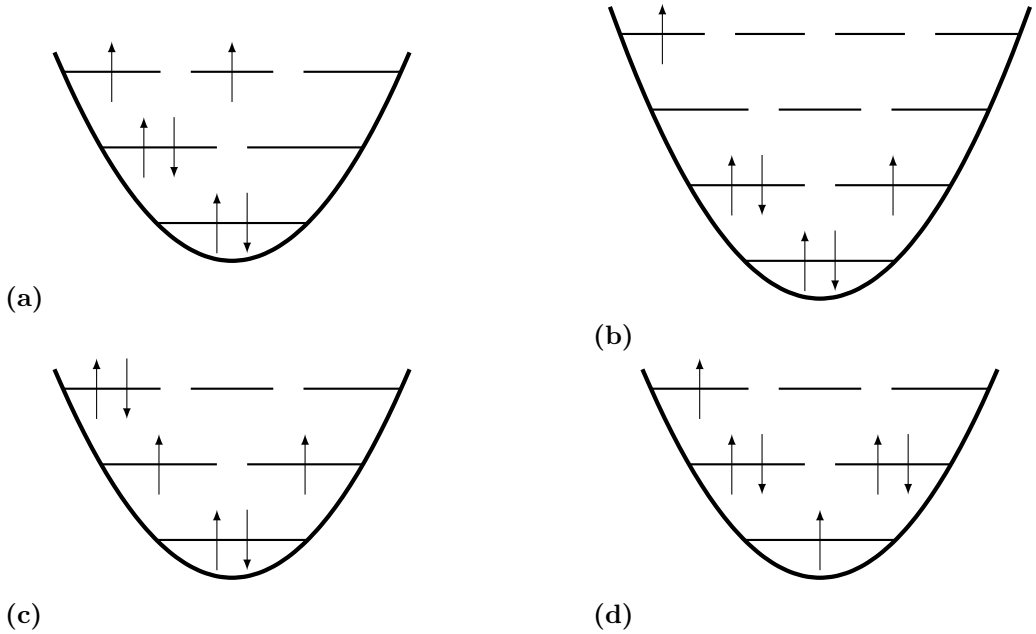

Figure 2.4: Four additional first excited states can be obtained by splitting pairs.

2.4.5 The degenerate case

In this section, the Richardson method will be used to solve the pairing Hamiltonian for potentials with degenerate single-particle spectra, a category in which multi-dimensional systems are included. Consider the Hamiltonian (2.42) generalised to degenerate single particle spectra

$$H = \sum_{j=1}^{n}\sum_{m}\varepsilon_j\left(a^\dagger_{jm}a_{jm} + a^\dagger_{j\bar{m}}a_{j\bar{m}}\right) - g\sum_{i=1}^{n}\sum_{j=1}^{n}\left(\sum_{m_1}a^\dagger_{jm_1}a^\dagger_{j\bar{m}_1}\right)\left(\sum_{m_2}a_{j\bar{m}_2}a_{jm_2}\right) \quad (2.64)$$

where m runs over the Ω_j degenerate states at each j, extending (2.42) to degenerate spectra. The summed pair operators are defined by

$$A_j = \sum_m b_{jm} \qquad A_j^\dagger = \sum_m b_{jm}^\dagger \tag{2.65}$$

where $b_{jm}^\dagger$ and single pair operators defined as earlier but extended by the additonal quantum number m

$$b_{jm} = a_{j\bar{m}} a_{jm} \qquad b_{jm}^\dagger = a_{jm}^\dagger a_{j\bar{m}}^\dagger \tag{2.66}$$

which have generalised versions of the hard-core boson commutation relations introduced in (2.44)

$$\left[b_{im_1}, b_{jm_2}^\dagger\right] = \left(1 - 2b_{jm_1}^\dagger b_{jm_1}\right)\delta_{ij}\delta_{m_1 m_2}. \tag{2.67}$$

The commuation relations of the summed pair operators follows from using their definitions

$$\left[A_i, A_j^\dagger\right] = \sum_{m_1}\sum_{m_2}\left[b_{im_1}, b_{jm_2}^\dagger\right] = \sum_{m_1}\sum_{m_2}(\Omega_j - 2b_{jm_1}^\dagger b_{jm_1})\delta_{ij}\delta_{m_1 m_2} = \left(\Omega_j - 2\sum_m b_{jm}^\dagger b_{jm}\right)\delta_{ij}. \tag{2.68}$$

Using the summed pair operators, the Richardson operators

$$B_J^\dagger = gC_J^* \sum_{j=1}^n \frac{A_j^\dagger}{2\varepsilon_j - E_J} \qquad B_J = gC_J \sum_{j=1}^n \frac{A_j}{2\varepsilon_j - E_J} \tag{2.69}$$

and

$$B_0 = \sum_{j=1}^n A_j \qquad B_0^\dagger = \sum_{j=1}^n A_j^\dagger \tag{2.70}$$

can be defined. The restricted Hamiltonian can be written with these operators as

$$H_{\mathcal{U}} = \sum_{j=1}^n \sum_m 2\varepsilon_j b_{jm}^\dagger b_{jm} - gB_0^\dagger B_0, \tag{2.71}$$

similar to the non-degenerate form previously introduced in equation (2.62). The state $|\psi\rangle$ is now required to be an eigenstate of $H_{\mathcal{U}}$, which is evaluated to

$$\begin{aligned} H_U|\psi\rangle =& H_U \prod_{\nu=1}^M B_{J_\nu}^\dagger |\psi\rangle = \left[H_U \prod_{\nu=1}^M, B_{J_\nu}^\dagger\right]|0\rangle \\ =& \sum_{\nu=1}^M \left(\left(\prod_{\mu=1}^{\nu-1} B_{J_\mu}^\dagger\right)[H_U, B_{J_\nu}^\dagger]\left(\prod_{\eta=\nu+1}^M B_{J_\eta}^\dagger\right)\right)|0\rangle . \end{aligned} \tag{2.72}$$

The commutator $[H_U, B_{J_\nu}^\dagger]$ evaluates to

$$\begin{aligned} \left[H_{\mathcal{U}}, B_J^\dagger\right] =& \sum_{j=1}^n 2\varepsilon_j \left[\sum_m b_{jm}^\dagger b_{jm}, B_J^\dagger\right] - gB_0^\dagger\left[B_0, B_J^\dagger\right] \\ =& \sum_{j=1}^n \left(E_J + gC_J B_0^\dagger \left(1 - g\sum_{j=1}^n \frac{\Omega_j - 2\sum_m b_{jm}^\dagger b_{jm}}{2\varepsilon_j - E_J}\right)\right) \end{aligned} \tag{2.73}$$

since

$$\begin{aligned}\left[\sum_m b_{jm}^\dagger b_{jm}, B_J^\dagger\right] =& gC_J \sum_{i=1}^{n}\sum_m \frac{b_{jm}^\dagger \left[b_{jm}, A_i^\dagger\right]}{2\varepsilon_i - E_J} = gC_J \sum_m \frac{b_{jm}^\dagger \left(1 - 2b_{jm}^\dagger b_{jm}\right)}{2\varepsilon_j - E_J} \\ =& gC_J \frac{A_j^\dagger}{2\varepsilon_j - E_J}\end{aligned} \tag{2.74}$$

and

$$\left[B_0, B_J^\dagger\right] = gC_J \sum_{i=1}^{n}\sum_{j=1}^{n} \frac{\left[A_i, A_j^\dagger\right]}{2\varepsilon_j - E_J} = gC_J \sum_{j=1}^{n} \frac{\Omega_j - 2\sum_m b_{jm}^\dagger b_{jm}}{2\varepsilon_j - E_J}. \tag{2.75}$$

This means that

$$\begin{aligned}H_{\mathcal{U}} |\psi\rangle =& \sum_{\nu=1}^{M} E_{J_\nu} \left(\prod_{\mu=1}^{M} B_{J_\mu}^\dagger\right) |0\rangle \\ &+ \sum_{\nu=1}^{M} gC_{J_\nu} \left(\prod_{\mu=1}^{\nu-1} B_{J_\mu}^\dagger\right) B_0^\dagger \left(1 - g\sum_{j=1}^{n} \frac{\Omega_j - 2\sum_m b_{jm}^\dagger b_{jm}}{2\varepsilon_j - E_J}\right) \left(\prod_{\eta=\nu+1}^{M} B_{J_\eta}^\dagger\right) |0\rangle \\ &= \mathcal{E} |\psi\rangle + gC_{J_\nu} \sum_{\nu=1}^{M} \left(1 - \sum_{j=1}^{n} \frac{g\Omega_j}{2\varepsilon_j - E_{J_\nu}}\right) B_0^\dagger \left(\prod_{\mu=1,\mu\neq\nu}^{M} B_{J_\mu}^\dagger\right) |0\rangle + \\ &gC_{J_\nu} \sum_{\nu=1}^{M} \left(\left(\prod_{\mu=1}^{\nu-1} B_{J_\mu}^\dagger\right) \left(\sum_{j=1}^{n} \frac{2B_0^\dagger \sum_m b_{jm}^\dagger b_{jm}}{2\varepsilon_j - E_{J_\nu}}\right) \left(\prod_{\eta=\nu+1}^{M} B_{J_\eta}^\dagger\right)\right) |0\rangle\end{aligned} \tag{2.76}$$

where $\mathcal{E} = \sum_{\nu=1}^{M} E_{J_\nu}$ is the energy of $|\psi\rangle$. Evaluating the final necessary commutator

$$\begin{aligned}[2g^2 C_I \sum_{j=1}^{n} \frac{B_0^\dagger \sum_m b_{jm}^\dagger b_{jm}}{2\varepsilon_j - E_I}, B_J^\dagger] =& 2g^2 C_I B_0^\dagger \sum_{j=1}^{n} \frac{\left[\sum_m b_{jm}^\dagger b_{jm}, B_J^\dagger\right]}{2\varepsilon_j - E_I} \\ =& 2g^2 C_I C_J B_0^\dagger \sum_{j=1}^{n} \frac{A_j^\dagger}{(2\varepsilon_j - E_I)(2\varepsilon_j - E_J)} \\ =& 2gC_I C_J B_0^\dagger \sum_{j=1}^{n} \frac{A_j^\dagger}{E_I - E_J} \left(\frac{1}{2\varepsilon_j - E_I} - \frac{1}{2\varepsilon_j - E_J}\right) \\ =& 2gB_0^\dagger \frac{gC_J B_I^\dagger - gC_I B_J^\dagger}{E_I - E_J}\end{aligned} \tag{2.77}$$

one can deduce by the calculation

$$
\begin{aligned}
&gC_{J_\nu}\sum_{\nu=1}^{M}\left(\left(\prod_{\mu=1}^{\nu-1}B_{J_\mu}^\dagger\right)\left(\sum_{j=1}^{n}\frac{2B_0^\dagger\sum_m b_{jm}^\dagger b_{jm}}{2\varepsilon_j-E_{J_\nu}}\right)\left(\prod_{\eta=\nu+1}^{M}B_{J_\eta}^\dagger\right)\right)|0\rangle\\
=&\sum_{\nu=1}^{M}\left(\left(\prod_{\mu=1}^{\nu-1}B_{J_\eta}^\dagger\right)\sum_{\lambda=\nu+1}^{M}\left(\left(\prod_{\kappa=\nu+1}^{\lambda-1}B_{J_\kappa}^\dagger\right)2gB_0^\dagger\frac{gC_{J_\lambda}B_{J_\nu}^\dagger-gC_{J_\nu}B_{J_\lambda}^\dagger}{E_{J_\lambda}-E_{J_\nu}}\left(\prod_{\iota=\lambda+1}^{M}B_{J_\iota}^\dagger\right)\right)\right)\\
&\times\left(\prod_{\eta=\nu+1}^{M}B_{J_\eta}^\dagger\right)|0\rangle\\
=&\sum_{\mu=1}^{M}\sum_{\nu=1}^{\mu-1}gC_{J_\mu}\frac{2g}{E_{J_\nu}-E_{J_\mu}}B_0^\dagger\left(\prod_{\eta=1,\eta\neq\mu}^{M}B_\eta^\dagger\right)|0\rangle-\sum_{\nu=1}^{M}\sum_{\mu=\nu+1}^{M}gC_{J_\nu}\frac{2g}{E_{J_\nu}-E_{J_\mu}}B_0^\dagger\left(\prod_{\eta=1,\eta\neq\nu}^{M}B_\eta^\dagger\right)|0\rangle\\
=&gC_{J_\nu}\sum_{\nu=1}^{M}\left(\sum_{\mu=1,\mu\neq\nu}^{M}\frac{2g}{E_{J_\mu}-E_{J_\nu}}\right)B_0^\dagger\left(\prod_{\eta=1,\eta\neq\nu}^{M}B_{J_\eta}^\dagger\right)|0\rangle
\end{aligned}
\tag{2.78}
$$

that the Hamiltonian evaluated on a state $|\psi\rangle$ built out of the Richardson operators results in

$$
H_{\mathcal{U}}|\psi\rangle=\mathcal{E}|\psi\rangle+gC_{J_\nu}\sum_{\nu=1}^{M}\left(1-g\sum_{j=1}^{n}\frac{\Omega_j}{2\varepsilon_j-E_{J_\nu}}+\sum_{J_\mu\neq J_\nu}^{M}\frac{2g}{E_{J_\mu}-E_{J_\nu}}\right)B_0^\dagger\left(\prod_{\substack{\eta=1\\\eta\neq\nu}}^{M}B_{J_\eta}^\dagger\right)|0\rangle\,. \tag{2.79}
$$

This yields the degenerate Richardson equations

$$
\frac{1}{g}-\sum_{j=1}^{n}\frac{\Omega_j}{2\varepsilon_j-E_{J_\nu}}+\sum_{J_\mu\neq J_\nu}^{M}\frac{2}{E_{J_\mu}-E_{J_\nu}}=0, \tag{2.80}
$$

which can easily be extended to include blocked levels by subtracting them from the degeneracy number Ω_j and substituting $\Omega_j\to\Omega_j-s_j$. These equations were first derived in their non-degenerate form by R.W. Richardson in 1963 [3]. Compared to the bosonic equations (2.59), there is an extra fermionic term present, which introduces a divergence when two energies are identical. While the Hamiltonian eigenvalue $\mathcal{E}$ is required to be real, there is no such requirements for the M individual pair energies E_{J_ν}. In fact, it will later be shown in the numerics that some of the E_{J_ν} will be required to have an imaginary part in order for the divergence to be resolved. Note also that the Richardson equations are valid for both repulsive and attractive interactions, although this work is restricted to attractive.

2.4.6 Generating initial values

To solve the Richardson equations (2.80) for an arbitrary state, one first needs to generate an initial set $\{E_{J_\nu}\}$ of solutions in the non-interacting case. In general this requires some thought, but for the ground state of a non-degenerate spectrum this

can simply be done by filling from the bottom up until M pairs have been filled. The production of the excited states are a bit more involved and depends on the spectrum of the theory, as was discussed in section 2.4.4.

For the purposes of solving the Richardson equations, the method of filling from the bottom up can also be used for the two-dimensional harmonic oscillator, disregarding the degeneracy by using the $A_j^\dagger$ operators. If two initial E_J end up having the same value, the Richardson equations will be divergent and the identical energies must be separated on the imaginary axis. This needs to be done in a symmetric way in order for the physical energy to stay real, and the procedure for this will be discussed in section 3.1.2.

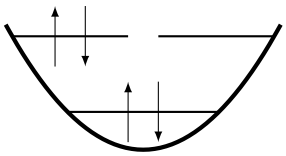

(a) The first of two degenerate ground states of the 2 pair two-dimensional harmonic oscillator.

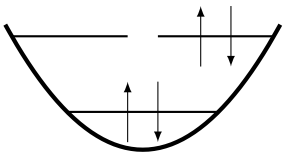

(b) The second of two degenerate ground states of the 2 pair two dimensional harmonic oscillator.

Figure 2.5: Two degenerate ground states of the two-dimensional harmonic oscillator occupied by two pairs. The two states will generate identical Richardson equations.

The degenerate theory introduces an additional complexity for the connection between a state in the non-interacting theory and states in the interacting theory assembled from the Richardson operators. Consider states of the types shown in figure 2.5. In the non-degenerate case, the procedure for obtaining the initial values for the Richardson energies E_{J_ν} is simply taking $E_{J_\nu} = 2\varepsilon_{J_\nu}$. In the degenerate case, the states will yield the same initial Richardson energies if this procedure is followed. The question arises which of the states the Richardson equations solve for, and it can be answered by considering the Richardson equations in the limit where the Richardson energies approach the non-interacting pair energies. Such a setup means letting $E_{J_\nu} = 2\varepsilon_{J_\nu} - \delta$ and taking the limit $\delta \to 0$ which gives

$$|\psi\rangle = \prod_{\nu=1}^{M} B_{J_\nu}^\dagger |0\rangle = \prod_{\nu=1}^{M} gC_{J_\nu} \sum_{j=1}^{n} \frac{A_j^\dagger}{\delta + 2(\varepsilon_j - \varepsilon_{J_\nu})} |0\rangle \longrightarrow_{\delta\to 0} \prod_{\nu=1}^{M} \frac{A_{J_\nu}^\dagger}{\sqrt{\Omega_{J_\nu}}} |0\rangle \tag{2.81}$$

which one recognises as a normalised superposition of the degenerate states.

2.4.7 Renormalisation of the coupling constant

When a large number of single-particle levels n is considered in (2.80), a problem that may arise is that the sum

$$\sum_{j=1}^{n} \frac{\Omega_j}{2\varepsilon_j - E_J} \tag{2.82}$$

will have an ultraviolet divergence when the free field spectrum ε_j is linear or lower order in j. This is the case in the physically interesting case of the harmonic oscillator. To counteract this divergence, one can introduce a renormalised interaction strength g' that is dependent on the level cutoff. Expanding the sum in the limit where $\varepsilon_j \gg E_J$, we have

$$\frac{\Omega_j}{2\varepsilon_j - E_J} = \frac{\Omega_j}{2\varepsilon_j} - \frac{\Omega_j}{(2\varepsilon_j)^2} E_J + ... \tag{2.83}$$

In the case of the two-dimensional harmonic oscillator with no blocked levels, the degeneracy of level j is $\Omega_j = j$, and the energies are also $\varepsilon_j \propto j$. This means that the zeroth order term is simply a constant while the linear order term has logarithmic ultraviolet divergence. This constitutes a problem since the interaction strength cannot be made to depend on E_J and the logarithmic divergence cannot be removed. Regardless, the interaction strength can be redefined to remove the linear divergence

$$\frac{1}{g'} = \frac{1}{g} + \sum_{j=1}^{n} \frac{\Omega_j}{2\varepsilon_j} \tag{2.84}$$

In the two-dimensional harmonic oscillator, the renormalisation term will simply be $n/(2\hbar\omega)$. Note that other single particle spectra may be completely renormalisable, as is the case for the infinite square well.

2.5 Further possibilities in Richardson models

To showcase the broad array of possibilities available in Richardson models, this section lists some of the situations it can be applied to.

2.5.1 Zeeman splitting by external magnetic field

If the particles are subject to an external magnetic field, there is an additional Zeeman splitting of the states due do this interaction. Such a magnetic field can be included without complication to the Richardson model by modifying the Hamiltonian (2.42) to

$$H = \sum_{j=1}^{n} \left[(\varepsilon_j + h)\, a_{j+}^\dagger a_{j+} (\varepsilon_j - h)\, a_{j-}^\dagger a_{j-} \right] - g \sum_{i=1}^{n} \sum_{j=1}^{n} a_{i+}^\dagger a_{i-}^\dagger a_{j-} a_{j+} \tag{2.85}$$

where h is the energy shift caused by the magnetic field. As this modification only concerns $\mathcal{U}^c$, the Richardson equations are unchanged by this modification and all one must do is to take into account the spin of particles when calculating the total energies of the system. As this will only contribute to a fine splitting, this has been excluded from further investigation for now.

2.5.2 Anisotropy of the potential

In this section, the effects of anisotropy of the potential on the Richardson solutions will be discussed. Consider as a simple example of this an anisotropic two dimensional harmonic oscillator with spectrum $\varepsilon_{ij} = \hbar\omega[\gamma^2(i - \frac{1}{2}) + \frac{1}{\gamma^2}(j - \frac{1}{2})]$. This will lift the degeneracy of the spectrum, once again reducing to the non-degenerate case. If the anisotropy is small, the same effects as in the degenerate case should be observed, and indeed the numerically obtained spectrum of figure 4.4b confirms this for the two-dimensional harmonic oscillator.

2.5.3 Repulsive interaction

It should be noted that the Richardson equations are equally valid for repulsive interactions as attractive interactions. In figure 3.11, the Richardson solutions are plotted not only for attractive but also for repulsive pairing interactions. One observes similar behaviour in the repulsive branch to the attractive branch.

3
Methods

3.1 Solving the Richardson equations

In this section, the methods employed to solve the Richardson equations in various interesting cases will be discussed. Restating the Richardson equations from equation (2.80) again, they are

$$\frac{1}{g} - \sum_{j=1}^{n} \frac{\Omega_j}{2\varepsilon_j - E_{J_\nu}} + \sum_{J_\mu \neq J_\nu}^{M} \frac{2}{E_{J_\mu} - E_{J_\nu}} = 0. \tag{3.1}$$

3.1.1 Recasting the Richardson equations

The equations (3.1) are singular when two pair energies E_{J_ν} merge. Other than the case of the initial values, this does indeed turn out to be the case as g is increased, as well as when initial values coincide in the degenerate case. To break the degeneracy, one can let the degenerate E_{J_ν} separate on the imaginary axis. This constitutes no problem for the physical energy of the system $\mathcal{E}$ as long as the sum over all E_{J_ν} remains real. As a way to handle the complex numbers in the numerics, one can explicitly notarise E_{J_ν} as complex numbers, writing

$$E_{J_\nu} = \xi_{J_\nu} + i\eta_{J_\nu} \tag{3.2}$$

which turns the Richardson equations into

$$\begin{aligned} &\frac{1}{g} - \sum_{j=1}^{n} \frac{\Omega_j}{2\varepsilon_j - \xi_{J_\mu} - i\eta_{J_\mu}} + \sum_{J_\mu \neq J_\nu}^{M} \frac{2g}{\xi_{J_\mu} + i\eta_{J_\mu} - \xi_{J_\nu} - i\eta_{J_\nu}} = 0 \quad \Rightarrow \\ &\frac{1}{g} - \sum_{j=1}^{n} \Omega_j \frac{2\varepsilon_j - \xi_{J_\nu} + i\eta_{J_\nu}}{(2\varepsilon_j - \xi_{J_\nu})^2 + \eta_{J_\nu}^2} + 2 \sum_{J_\mu \neq J_\nu}^{M} \frac{(\xi_{J_\mu} - \xi_{J_\nu}) - i(\eta_{J_\mu} - \eta_{J_\nu})}{(\xi_{J_\mu} - \xi_{J_\nu})^2 + (\eta_{J_\mu} - \eta_{J_\nu})^2} = 0 \end{aligned} \tag{3.3}$$

which split into a system of $2M$ equations

$$\begin{aligned} \frac{1}{g} - \sum_{j=1}^{n} \Omega_j \frac{2\varepsilon_j - \xi_{J_\mu}}{(2\varepsilon_j - \xi_{J_\mu})^2 + \eta_{J_\mu}^2} + 2 \sum_{J_\mu \neq J_\nu}^{M} \frac{\xi_{J_\mu} - \xi_{J_\nu}}{(\xi_{J_\mu} - \xi_{J_\nu})^2 + (\eta_{J_\mu} - \eta_{J_\nu})^2} = 0 \\ \sum_{j=1}^{n} \Omega_j \frac{\eta_{J_\mu}}{(2\varepsilon_j - \xi_{J_\mu})^2 + \eta_{J_\mu}^2} - 2 \sum_{J_\mu \neq J_\nu}^{M} \frac{\eta_{J_\mu} - \eta_{J_\nu}}{(\xi_{J_\mu} - \xi_{J_\nu})^2 + (\eta_{J_\mu} - \eta_{J_\nu})^2} = 0 \end{aligned} \tag{3.4}$$

for $2M$ real variables. To these equations, appropriate renormalisation terms can be added depending on the single particle spectrum.

3.1.2 Solution algorithm

The basic algorithm for solving these equations is then the following. One first decides on an initial occupation, and lets the initial values E_{J_ν} start out with the corresponding energies, using the procedure discussed earlier. Starting from this the coupling constant is then iteratively increased and the equations are solved in each step, using a modified Powell method [17] as implemented in the `scipy` [18] library. As the coupling constant increases, the solutions E_{J_ν} might start to approach each other, requiring the solver to start to separate them on the imaginary axis. The separation will always happen in complex conjugate pairs, which ensures that the physical energy $\mathcal{E}$ remains real. The process is then continued until the desired maximal coupling constant is reached.

The increasing of the coupling constant is done by increasing with a fixed percentage every step. If no solution is found, the initial values are adjusted slightly by adding Gaussian noise. This is then tried a number of times, and if a valid solution is still not found the step size is lowered and the procedure is tried again. Because of the fact that there are multiple solutions available at any given g and that the added Gaussian noise may have transitioned the solver to another solution family, the found solutions are first vetted before accepting them. This is done by rejecting any solution that has discontinuities in the physical energy $\mathcal{E}$ as well as it's derivative with respect to g.

When a solution has been found, the step size is increased back to its base value again, in order to minimise the number of iterations of the solver. A number of schemes to reset the step size was tried, but in the end it was found that simply resetting directly to the base value yielded good results.

A problem arises in the degenerate case when there are multiple initial E_{J_ν} starting at the same value with the second summation in the equations (3.4) diverging. This is solved by separating the n_D degenerate pair energies symmetrically on the imaginary axis, such that their sum remains real. A sketch of the distrubution of the imaginary parts is shown in figure 3.1. A numerical solver operating with the algorithm described has been developed in python with the critical parts of the code accelerated via JIT-compilation of the code through the `numba` library [19]. This library allows python code to be compiled into fast machine code, accelerating the solver by about a factor 10 compared to a pure pythonic implementation, with the difference only increasing for larger systems. Compared to exact diagonalisation of the Hamiltonian (2.42), solving the system (3.4) of non-linear equations is a computationally very cheap method to obtain equivalent results, with computationally feasible limit in the 100 pair range.

Some care has to be taken when selecting the single particle cutoff level n, which sets the number of single particle levels n_s. In the non-degenerate computations half-filling ($n_s = 2M$) was used. This fixes the ratio of filled states to total states $\frac{M}{n_s}$ to $\frac{1}{2}$, and allows for comparing results obtained with multiple system sizes. Generalising this to the two-dimensional harmonic oscillator, taking the single-particle

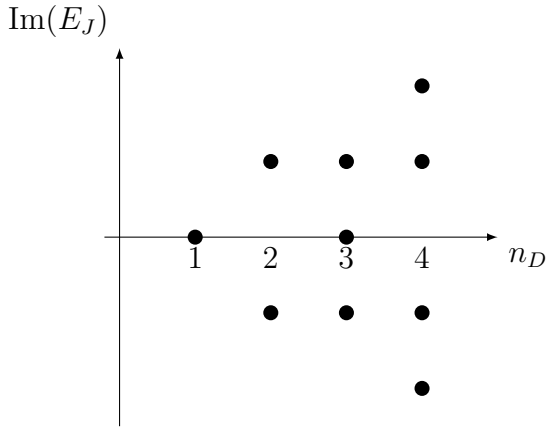

Figure 3.1: A sketch of the distribution of the initial values on the imaginary axis for n_D degenerate initial energies.

cutoff shell to be twice that of the highest filled shell will yield the fraction

$$\frac{M}{n_s} = \frac{\frac{1}{2}\Gamma(\Gamma+1)}{\frac{1}{2}2\Gamma(2+1)} = \frac{1}{2}\frac{\Gamma+1}{2\Gamma+1} \xrightarrow[\Gamma\to\infty]{} \frac{1}{4} \tag{3.5}$$

where Γ is the highest filled shell. While this fraction is not fixed for all system sizes, it does have a well-defined limit. The deviation from this limit is already < 10 % at $\Gamma = 5$. This means that the cutoff ratio can essentially be considered fixed for all but the smallest systems. Note that in the experimental context of harmonically trapped atoms, there is actually a physical motivation of the cutoff in that the trap potential has finite wall height and thus cannot accommodate an infinite number of single-particle states.

To illustrate the capabilities of the solution algorithm, the following sections will contain examples of systems it has been applied to.

3.2 Bosonic solutions

Initially the numerical solver was employed to solve the bosonic Richardson equations (2.59). The solution for the fermionic ground state of $M = 6$ pairs at half-filling ($n = 2M$) in the harmonic oscillator is shown in 3.2. For the bosonic case, there is no merging of the energies for the fermionic ground state. It should be noted that this is a highly excited state for bosons, and the bosonic ground state is also included for reference. As the bosonic equations are fully convergent when Richardson energies are identical, the solutions do not acquire an imaginary part. Note that the plots are drawn with both the interaction strength and the Richardson energies being measured in units of the single particle level gap, $\hbar\omega$. All of the following results have been obtained using this unit convention.

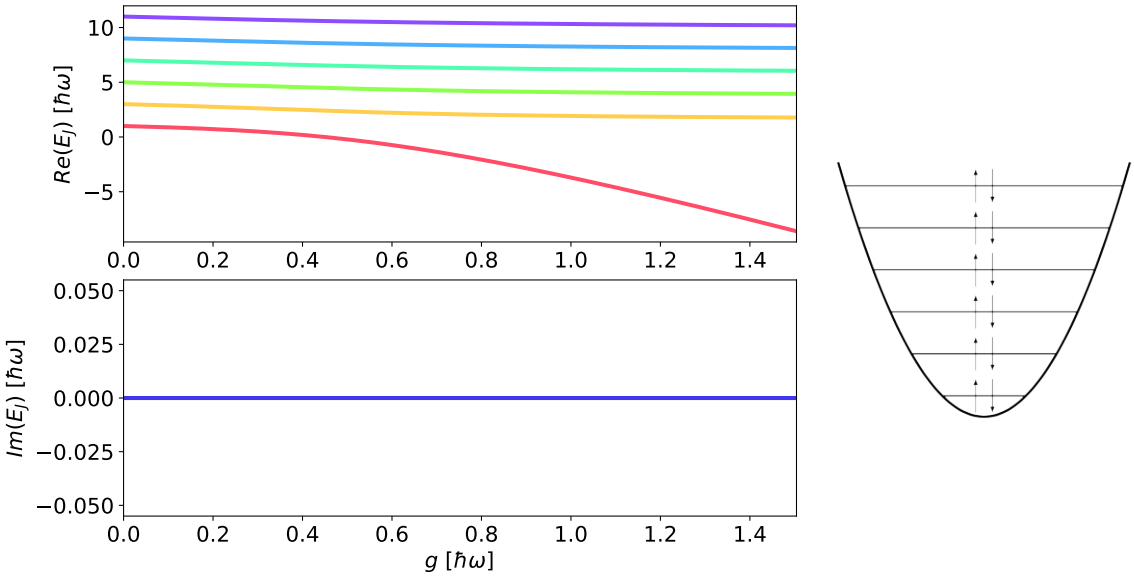

Figure 3.2: The Richardson solutions for the fermionic ground state and the bosonic ground state of 6 bosonic pairs in the one-dimensional harmonic oscillator at half-filling.

3.3 Fermionic solutions

The fermionic term was then included in the equations to obtain a solution for the ground state of $M = 6$ pairs of fermions at half-filling in the harmonic oscillator, shown in figure 3.3. Unlike in the bosonic case, the pair energies now start to merge with ascending g in order of descending non-interacting energies.

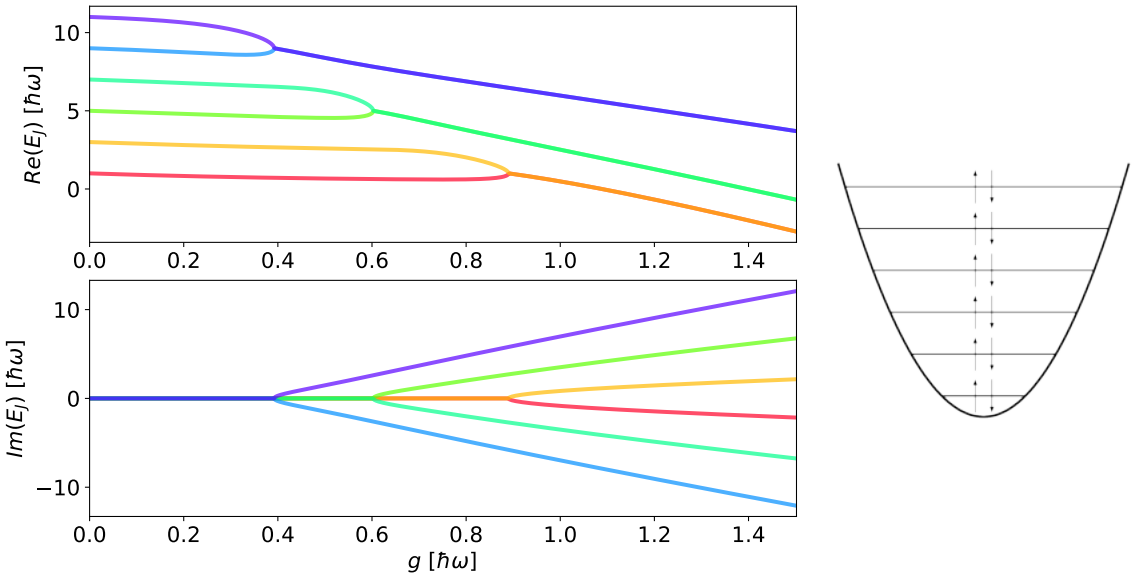

Figure 3.3: The Richardson solutions for the ground state of 6 fermionic pairs in the one-dimensional harmonic oscillator at half-filling.

The first excited state of the same 6 pair system is plotted in figure 3.4. The

highest and lowest pair energies will now remain unmerged, with the highest energy remaining finite in the $g \to \infty$ limit.

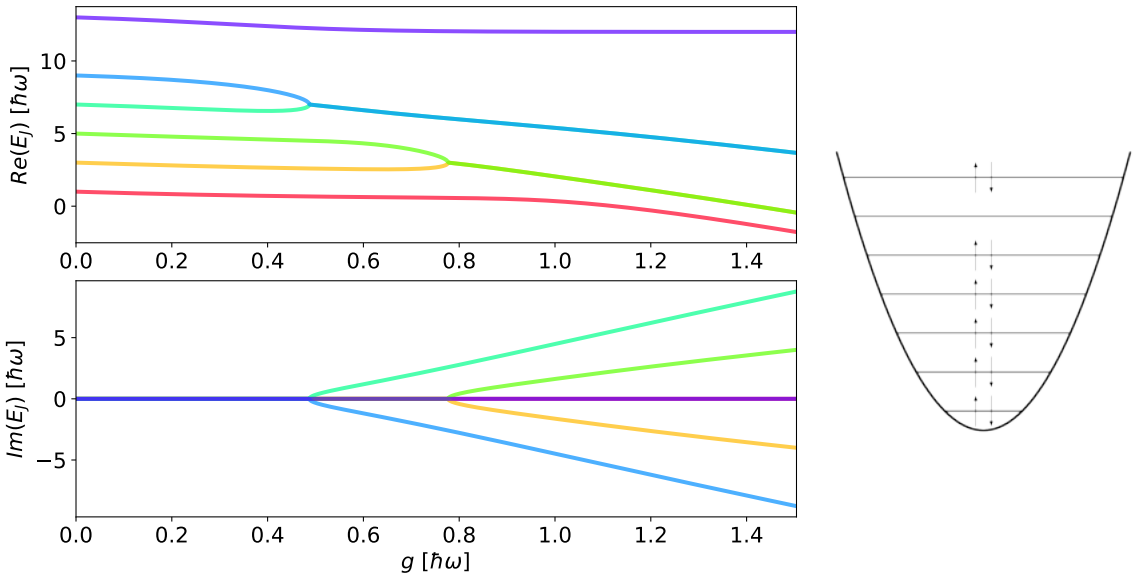

Figure 3.4: The Richardson solutions for the first excited state of 6 fermionic pairs in the one-dimensional harmonic oscillator at half-filling.

Solutions for using the infinite square well for the single particle spectrum instead of the harmonic oscillators are shown in figure 3.5, the single particle spectrum now being $\varepsilon_j = \hbar\omega j^2$. The infinite square well exhibits the same merging behaviour as the harmonic oscillator, with the main difference being that the interval between the merges now shrinks with increasing interaction strength.

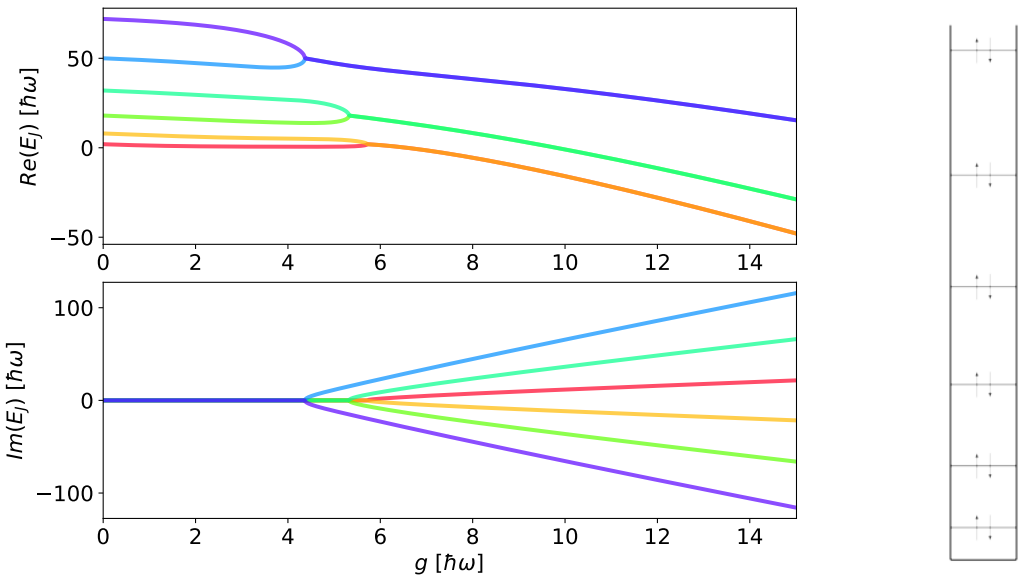

Figure 3.5: The Richardson solutions for 6 fermionic pairs in the one-dimensional infinite square well.

The energy spectrum of the 6-pair system for 6 of the lowest excited states is shown in figure 3.6. Here one can clearly observe that for a large interaction strength, the spectrum approaches the characteristic superconductor spectrum of one large gap from the ground state to the first excited state and then a virtually continuous spectrum. Unlike the result found in BCS theory, the spectrum is continued with a large gap and then being virtually continuous again. The coarse excitations are called elementary excitations and have been discussed in the literature [20] previously. Essentially the number of elementary excitations is equal to how many of the pair energies E_{J_ν} remain finite in the $g \to \infty$ limit, with figure 3.4 being an example of a state with a single elementary excitation. One additionally observes that the spectrum of excitation energies is unchanged for small g, reflecting the result that all M-particle states have the same change in energy found in the first order perturbation theory calculations of section 2.4.1.

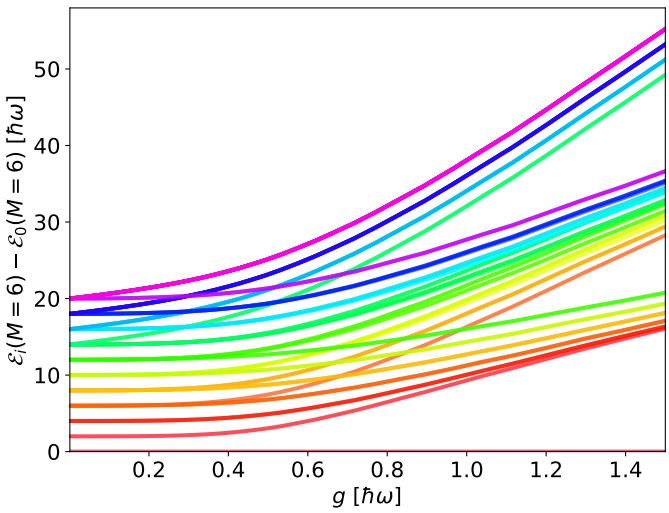

Figure 3.6: The excitaton energy spectrum for 6 fermionic pairs in the harmonic oscillator as a function of the interaction strength g.

To show the complicated merging behaviour displayed by the higher excited states of a larger number of interacting pairs, the solutions for a 20 pair excited state in the harmonic oscillator is displayed in figure 3.7. As can be seen, there is a series of merging and separation of the pair energies, and also a crossing of energies. The crossing is possible because two of the pair energies involved are merged and separated on the imaginary axis.

3.4 Degenerate solutions

The results of the solver applied to the 6 pair ground state in the two-dimensional harmonic oscillator is plotted in figure 3.8. This constitutes 3 fully filled shells.

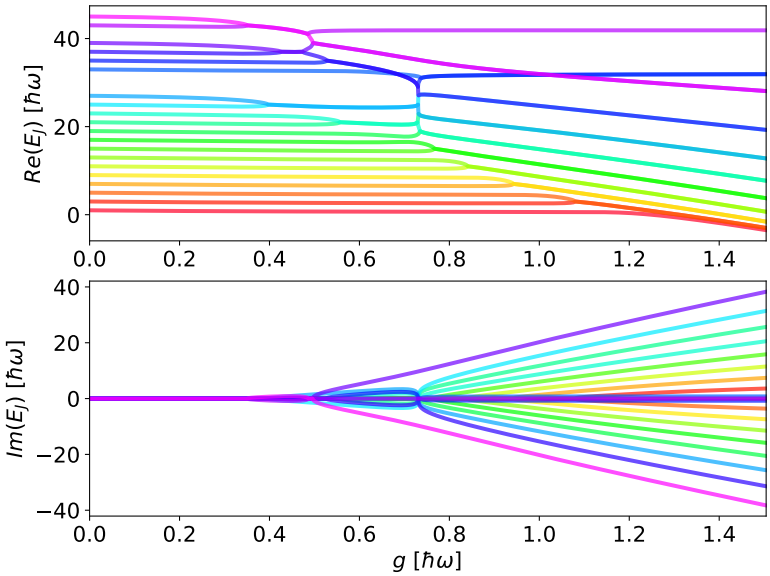

Figure 3.7: The Richardson solutions for a higher excited 20 pair state of 3 elementary excitations.

The pattern of merging now involves separations as well but as previously the more energetic states merge first.

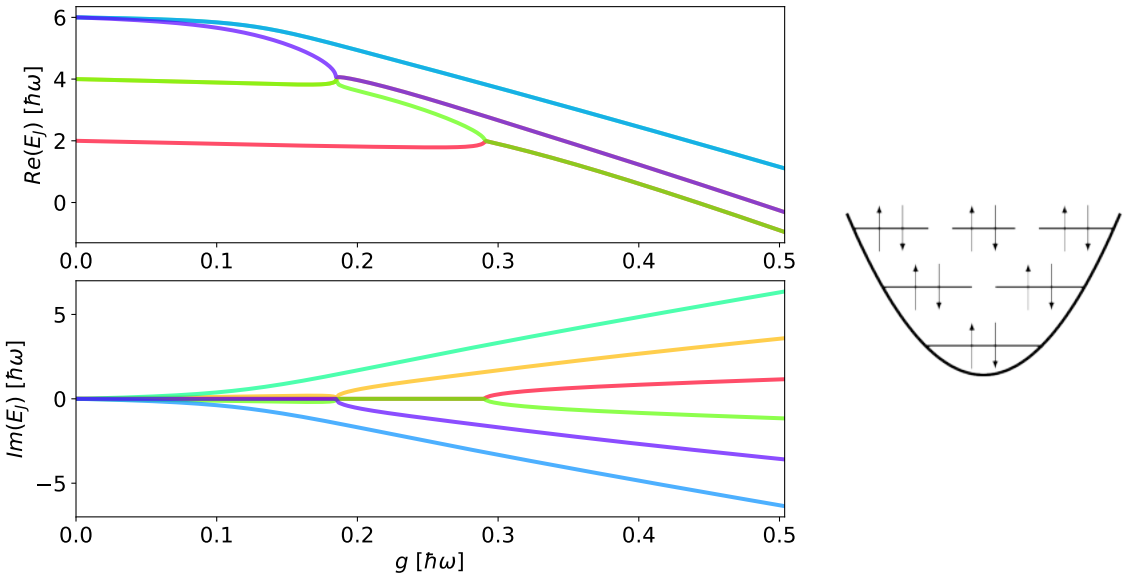

Figure 3.8: The Richardson solutions for the 6 pair ground state of the two dimensional harmonic oscillator.

Also interesting is the case of the two-dimensional infinite square well, which has a rather different pattern of degeneracy. A plot of the solutions for 6 pairs is shown in figure 3.9, as well as an occupation sketch. There are no major qualitative differences between the two and three-dimensional cases, as is illustrated in figure 3.10 which shows the ground state of the three dimensional harmonic oscillator with 10 pairs, which comprises 3 fully filled shells. One would not have expected any major

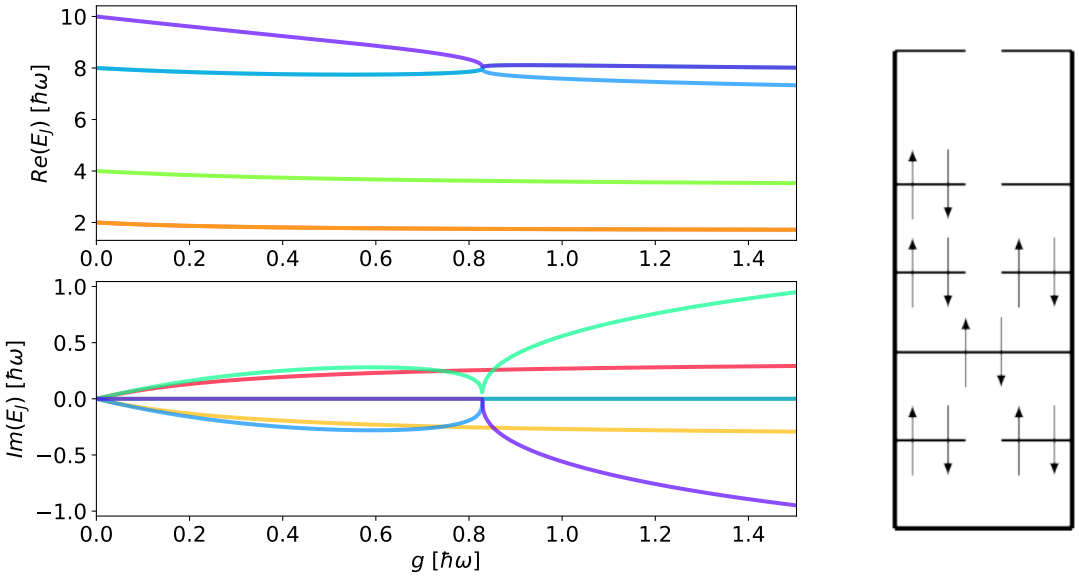

Figure 3.9: The Richardson solutions for the 6 pair ground state of the two dimensional infinite square well.

differences either, as the three dimensional harmonic oscillator only differs from the two dimensional in that the degeneration number is quadratic in j, being $\Omega_j = \frac{j(j+1)}{2}$ which simply results in more degenerate states at each level. While it may seem that the slight increasing of the highest Richardson energy is new behaviour, it is in fact present in the two-dimensional case for $\Gamma \geq 5$. As the degeneration number of the third shell of the three-dimensional harmonic oscillator is 6, a threshold of $\Omega_j = 5$ from which the highest Richardson energy will have a slight increase can be identified.

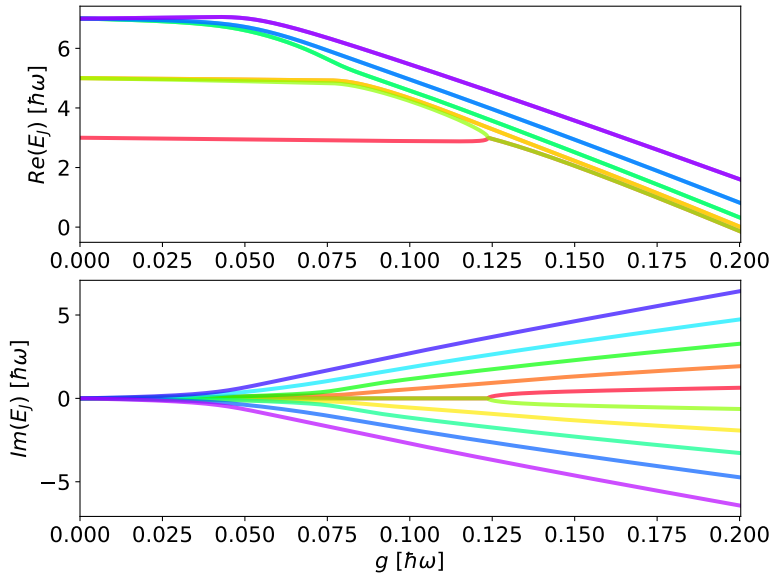

Figure 3.10: The Richardson solutions for the 10 pair ground state of the three dimensional harmonic oscillator.

3.4.1 The effects of renormalisation

In figure 3.11 the effects of renormalising the equations for 6 pairs in the two dimensional harmonic oscillator by removing the constant term as described in section 2.4.7 is shown. Note that the equations are still not fully convergent, as the logarithmically divergent term still remains. There is however a large difference to the non-renormalised result aside from the asymptotic deviation in that the merging of the states is smudged.

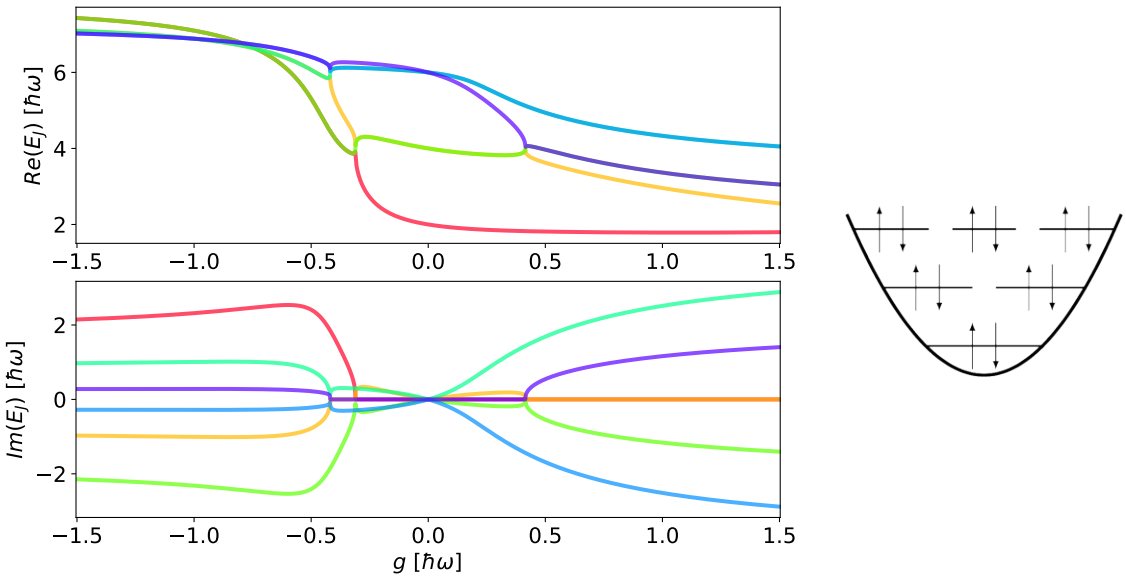

Figure 3.11: The renormalised Richardson solutions for the 6 pair ground state of the two dimensional harmonic oscillator, with the repulsive branch included.

The same plot also includes solutions for the repulsive branch of the interaction, which is also solvable with the Richardson equations. As can be seen, the repulsive branch also displays the merging behaviour observed in the attractive branch.

4

Results

4.1 Results for mesocopic superconductors

In this section some previously found results on mesoscopic superconductors will be reproduced numerically using the Richardson model developed here.

4.1.1 Condensation energy

As discussed in section 2.3, a parameter which has been studied in the literature for mesoscopic superconductors is the condensation energy, as defined in equation (2.37). The condensation energy is plotted in figure 4.1 for increasing level spacing divided by bulk energy gap $\hbar\omega/\Delta$, which implies shrinking the system. The result is quite different for an even and odd number of electrons. The BCS theory supplies the result $-\frac{\Delta^2}{2\hbar\omega}$, which is also plotted for comparison. Previous work [21] condsidered half-filled systems of equidistant levels $\varepsilon_j = \hbar\omega(j - \frac{1}{2})$ and a dimensionless interaction strength $\lambda = 0.224$, with $g = \hbar\omega\lambda$ giving $\hbar\omega/\Delta = 2\sinh\left(\frac{1}{\lambda}\right)/M$. The figure shows the discrepancy between the theories, with the Richardson result consistently lower than the bulk result. One expects that the theories agree in the bulk limit, i.e for $\hbar\omega/\Delta \to 0$. Here a crossover region can clearly be identified between the bulk and mesoscopic regime, and instead of the condensation energy going to zero as the BCS result it stabilises. Note that the maximum $\hbar\omega/\Delta$ in the plot corresponds to two pairs and that the condensation energy thus cannot be defined further to the right.

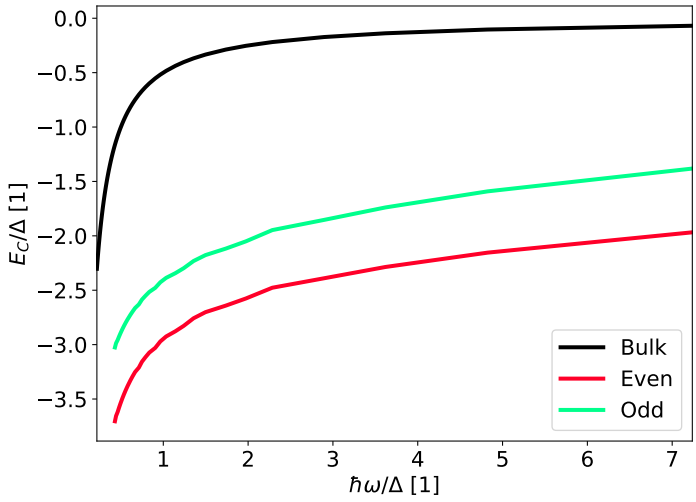

Figure 4.1: The condensation energy $E_C(N)/\Delta$ plotted against $\hbar\omega/\Delta = 2\sinh\left(\frac{1}{\lambda}\right)/M$ for $\lambda = 0.224$.

The results clearly indicates the importance of parity for the mesocopic systems, and the extended crossover regime indicates that some favourability of condensation remains even for the smallest systems. The evolution of the condensation energy can be understood from the asymptotic behaviour of the Richardson solutions of figure 3.3 by realising that the asymptotic descent starts after merges and that for larger systems, the first merges happen earlier. This in turn means that the total energy $\mathcal{E}$ starts to decrease for lower interaction strength g.

4.1.2 Matveev-Larkin parameter

The solver was also used to calculate the Matveev-Larkin parameter for a number of cases. Recalling the definition (2.39), the Matveev-Larkin parameter is

$$\Delta_{ML}(N) = \mathcal{E}_G(N) - \frac{1}{2}\left[\mathcal{E}_G(N+1) + \mathcal{E}_G(N-1)\right] \tag{4.1}$$

where N is an odd integer and denotes the number of particles in the system. It should thus be clear that the Matveev-Larkin parameter is defined as the difference between the energy of the system with an upaired particle and the mean of the energy of neighbouring fully paired states. A plot of the energies $\mathcal{E}_G(N)$ for a small number of particles in the harmonic oscillator is shown in figure 4.2. Here the value of the Matveev-Larkin parameter is the height of the dashed red lines. As can be observed, the Matveev-Larkin parameter increases with the interaction strength and with the number of particles, and is naturally only non-zero for odd particle numbers. The theoretical prediction of a minimum discussed in section 2.3 is confirmed, being more apparent for the greater interaction strengths.

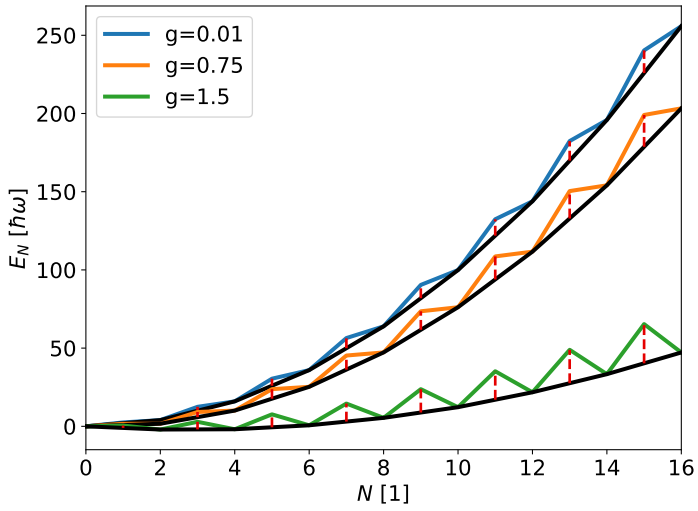

Figure 4.2: The ground state energies E_N is shown here for various g plotted as a function of N. The Matveev-Larkin parameter Δ_{ML} is shown as the dashed red lines.

4.2 Results for harmonically trapped atoms

In this chapter, the degenerate solver will be applied to the case of a number of atoms trapped in a two-dimensional harmonic oscillator.

4.2.1 Excitation spectrum

Using the solver, excitation spectra of two-dimensional harmonic oscillator systems of various sizes were able to be obtained. Spectra of the first excitations for $N = 6$ and $N = 72$ is shown in figure 4.3. Here one sees how the degenerate excitations in the free theory are separated in the interacting theory. The existence of an extremum for the excitation energy for some excitations is a feature unable to be obtained from perturbation theory. Note that all of the results obtained here are calculated with the cutoff scheme described in section 3.1.2. The spectra show the excitation energy, defined as

$$\Delta E_{i,0}(N) = \mathcal{E}_i(N) - \mathcal{E}_0(N)$$

which in the non-interacting theory is fixed to 2 for all types of first excited states. As the interaction is turned on, the degeneracy in the excitation energy is lifted and the spectrum splits. Of the excited states plotted in figure 4.3, the ones with an increasing excitation energy are the ones created by breaking a pair and exciting single particles to either the first or second excited level.

In figure 4.4, the excitation energy of the first pair excitation is shown as a function of g for various numbers of pairs M. From figure 4.4a, one observes a minimum of the excitation energy for a critical value of the interaction strength, g_{crit}. The

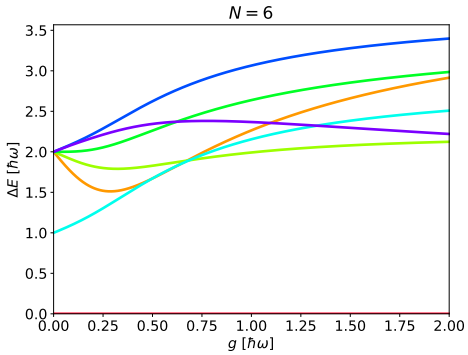

(a) The lowest excitation spectrum for a 6 particle system.

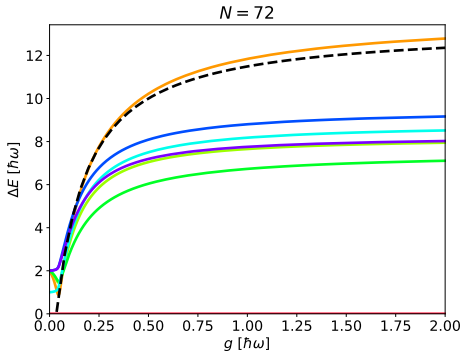

(b) The lowest excitation spectrum for a 72 particle system.

Figure 4.3: The spectra of some of the lowest excitations for a 6 particle system (**a**) and a 72 particle system (**b**) in the two-dimensional harmonic oscillator.

minimal energy will be denoted ΔE_{min}. The figure 4.4b showcases the effect of introducing an anisotropy to the spectrum, with the anisotropic results shown as dashed and dotted lines respectively. As can be seen, the minima is observed for all system sizes in the slightly anisotropic case, with the value of ΔE_{min} being quite a bit higher than the corresponding values for the isotropic system. For a larger anisotropy, only the largest system with $M = 10$ retains the minima with the other systems having crossed over to the behaviour observed in the non-degenerate one-dimensional case. This would indicate that a slight anisotropy yields closing of the excitation gap for larger systems compared to the systems with isotropic spectra, and the presence of some critical anisotropy where the system crosses over to the monotonic case.

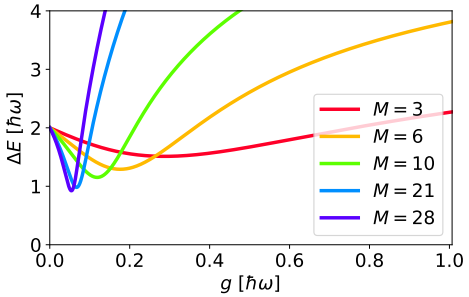

(a) The evolution of the first pair excitation energy ΔE for increasing numbers of interacting pairs M, as a function of interaction strength g. Note the location of the minima.

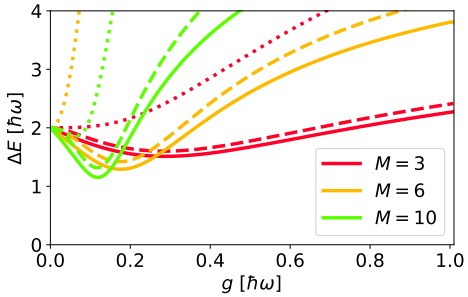

(b) The rescaled first pair excitation energies for isotropic ($\gamma = 1$, solid), slightly anisotropic ($\gamma = 1.01$, dashed) and anisotropic ($\gamma = 1.1$, dotted) single particle spectra.

Figure 4.4: The figure shows the first pair excitation energy for various system sizes, for both isotropic and anisotropic spectra.

Recalling the gap equation (2.35), it can be specialised to the two-dimensional har-

monic oscillator systems studied here by first expressing the summation at half-filling using the degeneration number Ω_j and taking $\Omega_j = j$. In the zero temperature regime, the chemical potential is equal to the Fermi energy which in the closed shell case of filling ratio (3.5) means that $\mu = \hbar\omega(\frac{n}{2} + \frac{3}{2})$. Substituting this into the gap equation, and taking into account the renormalisation of g, it becomes

$$\frac{1}{g} + \frac{n}{2} = \sum_{j=1}^{n} \frac{j}{2\sqrt{(j - (\frac{n}{2} + \frac{3}{2}))^2 + \Delta^2}}. \tag{4.2}$$

The gap equation can be solved for $\Delta = 0$ to obtain an approximate prediction of the critical interaction strength g_{crit} where the excitation gap is expected to go zero in the thermodynamic limit. The prediction is that

$$g_{\text{crit}} = \left(\sum_{j=1}^{n} \frac{j}{2|j - (\frac{n}{2} + \frac{3}{2})|} - \frac{n}{2} \right)^{-1} \tag{4.3}$$

which is where the dashed line of figure 4.3b starts. In a bulk BCS system, the energy required to excite a pair to the first excited level would be 2Δ. As the Richardson theory reduces to the BCS theory in the thermodynamic limit, the expectation is that the excitation energy produced by solving the Richardson equations should agree for large systems. The prediction from the bulk theory is smaller than the numerically obtained value, with the two values starting to align more for larger systems, reflecting that the thermodynamic limit is being approached.

Solving (4.3) as a function of n provides an estimate for the critical interaction strength which should agree with that obtained from solving the Richardson equations in the bulk limit. In figure 4.5, these solutions are plotted as the dashed black line, showing asympotic agreement with the results obtained from solving the Richardson equations for increasing number of fully filled shells Γ.

For the purpose of studying if the parity effects present in the one-dimensional systems play a part in the transition studied here, the Richardson equations are solved for both an even number of particles and an odd number of particles. The odd numbered systems are obtained by placing an unpaired particle in the unfilled shell directly above shell Γ. As can be observed from the plots of figure 4.5, while some parity dependence is found for the value of the minimal excitation energy ΔE_{min}, it is found to diminish for increasing system size but may still be possible to observe for small systems.

Returning to the previous discussion of the excitation energy for excitation of a pair to the next level, which is expected to go to zero in the many-body limit, one can study the quantities g_{crit} and ΔE_{min} as functions of system size in order to confirm or reject this hypothesis. This has been tested numerically by studying large systems, and figure 4.5 shows this for closed-shell configurations up to 17 fully filled shells, corresponding to 153 pairs. A power law was fit to the minimal excitation energy, revealing that the ΔE_{min} scales with the number with exponent $-4/10$. This is a novel prediction that should be able to be checked with trapped atom experiments

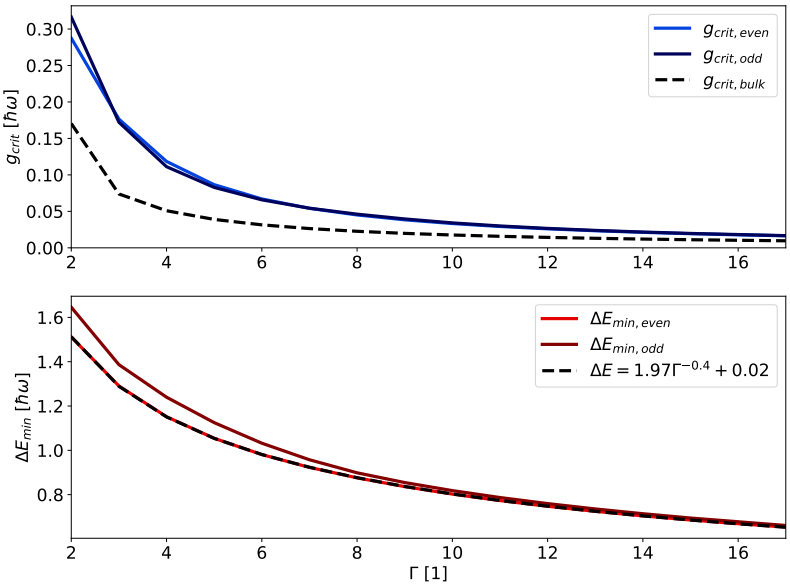

Figure 4.5: The evolution of the critical interaction strength and excitation energy as a function of increasing highest filled shell Γ.

of the kind used by Bayha *et al.* [7], if data could be obtained for larger number of particles.

5
Conclusion

5.1 The Richardson approach

This thesis has developed code for a solver capable of both generating initial values and solving the Richardson equations for general spectra and excitation levels. This allowed for reproducing previously obtained results with regards to the condensation energy and the Matveev-Larkin parameter.

Compared to previous work, the current solution algorithm allowed for solving the energies of models using degenerate single particle spectra, which produced new results for excitation spectra for interacting systems of various sizes. The ability to produce solutions for arbitrary excited states is also a benefit of the developed algorithm, which allows for studying a multitude of interesting problems.

The computational cost of running the solver must be considered in relation to the alternative methods of obtaining equivalent results. Of these methods, the only one which to the author's knowledge can produce these results is exact diagonalisation through for example the Lanczos algorithm. Compared to this, solving a system of non-linear equations is vastly computationally cheaper and considering also that the method produces exact results the Richardson approach is an attractive way of solving pairing problems with a broad set of possible applications. There is a very small number of physically interesting quantum models for interacting particles with exact solutions available which can resolve this many particles, which also makes Richardson models interesting from a theoretical standpoint in its own right.

5.2 Trapped atoms

Specifically for the context of harmonically trapped atoms, the Richardson approach has allowed for studying previously computationally unfeasible systems numerically. While this has not illuminated any previously unknown qualitative properties, it has enabled a description of the systems under consideration for previously inaccessible system sizes. Ultimately, this thesis includes results for systems of size up to 306 interacting particles.

Using these results, it has been possible to make a prediction for the scaling of the minimal excitation energy $\Delta E_{\min}$ as a function of the number of fully filled shells Γ as the exponent $-4/10$. This prediction should be able to be checked experimentally,

if the experiments are able to be conducted for larger number of particles.

5.3 Possibility of further research

There are a number of further interesting questions that are possible to study with the Richardson approach. In the section 2.5, some possible extensions to the model itself are mentioned. It should be noted that the Richardson approach is a very versatile tool for describing pairing problems, and even exact wavefuncitons are possible to obtain with the method. This enables the possibility of calculating transition matrix elements, which can be used to obtain lifetimes of excited states, which would be interesting to attempt to fit to experimental data.

There is also an interesting theoretical distinction between anisotropic systems and non-degenerate systems. As has been only briefly touched upon in this thesis, slightly anisotropic two-dimensional systems display similar spectral properties to fully degenerate ones. This is interesting as such a spectrum could be realised in 1D, with for example $\varepsilon_j = \hbar\omega[j + (1-\alpha)\sin(j/\beta)]$ being a case of a simulated two-dimensional anisotropic spectrum which could be studied. The crossover anisotropy would also be interesting to investigate in further study.

The system sizes presented in this thesis are in no way the computational limit of what is possible with Richardson models. By extending the code to distribute the evaluation of the Richardson equations over multiple cores, one would be able to increase the performance of the solver significantly and enable solving larger systems in feasible time. This was tried during the code development process, but the method used made the overhead too large for a net performance gain to be obtained. With a computational approach more suited to computational distribution from the beginning, it should no doubt be possible to find a large performance gain in this way.

Another possibility is to utilise the capability of the algorithm to obtain arbitrary excited states and study the thermodynamics of pairing systems using statistical mechanics. With such methods the temperature dependence of superconductivity could be studied, which would possible give new insights on the mesoscopic physics of superconducting systems.

Bibliography

[1] J. Bardeen, L. N. Cooper, and J. R. Schrieffer, "Theory of superconductivity," *Phys. Rev.*, vol. 108, pp. 1175–1204, Dec 1957.

[2] L. N. Cooper, "Bound electron pairs in a degenerate fermi gas," *Phys. Rev.*, vol. 104, pp. 1189–1190, Nov 1956.

[3] R. Richardson, "A restricted class of exact eigenstates of the pairing-force hamiltonian," *Physics Letters*, vol. 3, no. 6, pp. 277–279, 1963.

[4] P. Anderson, "Theory of dirty superconductors," *Journal of Physics and Chemistry of Solids*, vol. 11, no. 1, pp. 26–30, 1959.

[5] C. T. Black, D. C. Ralph, and M. Tinkham, "Spectroscopy of the superconducting gap in individual nanometer-scale aluminum particles," *Phys. Rev. Lett.*, vol. 76, pp. 688–691, Jan 1996.

[6] J. Dukelsky, S. Pittel, and G. Sierra, "Colloquium: Exactly solvable richardson-gaudin models for many-body quantum systems," *Rev. Mod. Phys.*, vol. 76, pp. 643–662, Aug 2004.

[7] L. Bayha, M. Holten, R. Klemt, K. Subramanian, J. Bjerlin, S. M. Reimann, G. M. Bruun, P. M. Preiss, and S. Jochim, "Observing the emergence of a quantum phase transition shell by shell," *Nature*, vol. 587, p. 583–587, Nov 2020.

[8] J. Bjerlin, S. Reimann, and G. Bruun, "Few-body precursor of the higgs mode in a fermi gas," *Physical Review Letters*, vol. 116, apr 2016.

[9] I. Bloch, J. Dalibard, and W. Zwerger, "Many-body physics with ultracold gases," *Rev. Mod. Phys.*, vol. 80, pp. 885–964, Jul 2008.

[10] K. H. Bennemann and J. B. Ketterson, *Superconductivity.* Springer, 2008.

[11] F. Han, *A Modern Course in the Quantum Theory of Solids.* World Scientific, 2013.

[12] I. Giaever, "Energy gap in superconductors measured by electron tunneling," *Phys. Rev. Lett.*, vol. 5, pp. 147–148, Aug 1960.

[13] J. von Delft, A. D. Zaikin, D. S. Golubev, and W. Tichy, "Parity-affected superconductivity in ultrasmall metallic grains," *Phys. Rev. Lett.*, vol. 77, pp. 3189–3192, Oct 1996.

[14] J. Dukelsky and G. Sierra, "Crossover from bulk to few-electron limit in ultrasmall metallic grains," *Phys. Rev. B*, vol. 61, pp. 12302–12314, May 2000.

[15] K. A. Matveev and A. I. Larkin, "Parity effect in ground state energies of ultrasmall superconducting grains," *Phys. Rev. Lett.*, vol. 78, pp. 3749–3752, May 1997.

[16] J. R. Bunch, C. P. Nielsen, and D. C. Sorensen, "Rank-one modification of the symmetric eigenproblem," *Numerische Mathematik*, vol. 31, no. 1, pp. 31–48, 1978.

[17] M. J. D. Powell, "An efficient method for finding the minimum of a function of several variables without calculating derivatives," *The Computer Journal*, vol. 7, pp. 155–162, 01 1964.

[18] P. Virtanen, R. Gommers, T. E. Oliphant, M. Haberland, T. Reddy, D. Cournapeau, E. Burovski, P. Peterson, W. Weckesser, J. Bright, S. J. van der Walt, M. Brett, J. Wilson, K. J. Millman, N. Mayorov, A. R. J. Nelson, E. Jones, R. Kern, E. Larson, C. J. Carey, İ. Polat, Y. Feng, E. W. Moore, J. VanderPlas, D. Laxalde, J. Perktold, R. Cimrman, I. Henriksen, E. A. Quintero, C. R. Harris, A. M. Archibald, A. H. Ribeiro, F. Pedregosa, P. van Mulbregt, and SciPy 1.0 Contributors, "SciPy 1.0: Fundamental Algorithms for Scientific Computing in Python," *Nature Methods*, vol. 17, pp. 261–272, 2020.

[19] S. K. Lam, A. Pitrou, and S. Seibert, "Numba: A llvm-based python jit compiler," in *Proceedings of the Second Workshop on the LLVM Compiler Infrastructure in HPC*, LLVM '15, (New York, NY, USA), Association for Computing Machinery, 2015.

[20] J. M. Román, G. Sierra, and J. Dukelsky, "Elementary excitations of the bcs model in the canonical ensemble," *Phys. Rev. B*, vol. 67, p. 064510, Feb 2003.

[21] J. von Delft and F. Braun, "Superconductivity in ultrasmall grains: Introduction to richardson's exact solution," 1999.

DEPARTMENT OF PHYSICS
CHALMERS UNIVERSITY OF TECHNOLOGY
Gothenburg, Sweden
www.chalmers.se

CHALMERS
UNIVERSITY OF TECHNOLOGY